Conference Proceedings

WIN SYMPOSIUM 2022 – ABSTRACT POSTER PRESENTATIONS

WIN Symposium 2022 – abstract poster presentations. *J Immunother Precis Oncol*. Published online. DOI: 10.36401/JIPO-22-X4.

SUMMARY

The WIN Symposium will take place on October 29-30, 2022 in Barcelona, Spain. The theme for this 2-day symposium is "Integrating genomics and transcriptomics to reshape precision oncology: A winning strategy." The WIN symposium 2022 poster abstracts will present a large panel of innovative concepts and technologies aimed at better understanding disease mechanisms, providing ideas and technologies for new biomarkers to improve efficacy of immunotherapies or combinations of immunotherapy with targeted therapy, and biomarkers allowing early detection of the disease and predictive of response to therapeutics.

A subset of posters provides an insight into novel therapeutic approaches, with novel targets supported by preclinical evidence with potential efficacy that could be candidates for clinical development.

Another subset of posters outlines the essential role of multi-omics approaches, combining Next Generation Sequencing, transcriptomics, proteomics, and bioinformatics, delineating an improvement in daily clinical practice. As representative examples:

- ALK translocations not detected by FISH have been characterized by NGS. RAS mutated cancers express different levels of mutated allele, with a level of mutated proteins comprised between 10% and 90%, with a substantial modulation of response to targeted therapies.
- Synergy between targeted therapies, immuno-therapies, radiation therapy and impact of chemotherapies on efficacy of immune response were presented with preclinical models and clinical studies.
- ALK translocations not detected by FISH have been characterized by NGS. RAS mutated cancers express different levels of mutated allele, with a level of mutated proteins comprised between 10% and 90%, with a substantial modulation of response to targeted therapies.

WIN Symposium 2022 poster abstracts are of high scientific quality. The presenters contribute to rich discussions with the audience and are instrumental to the success of the meeting.

Abstract No: 1

Beyond the tip of the iceberg: Proteomic analysis in colon and breast cancer

Gerald Batist, Connie Sobsey, Georgia Mitsa, Christoph Borchers

Segal Cancer Centre, Jewish General Hospital & McGill University Centre for Translational Research, Canada

Introduction: The WINTHER trial demonstrated the limitation of genome-only profiling to stratify patients and guide therapeutic matches. Transcriptome analysis expands the therapeutic targets, genomic data do not

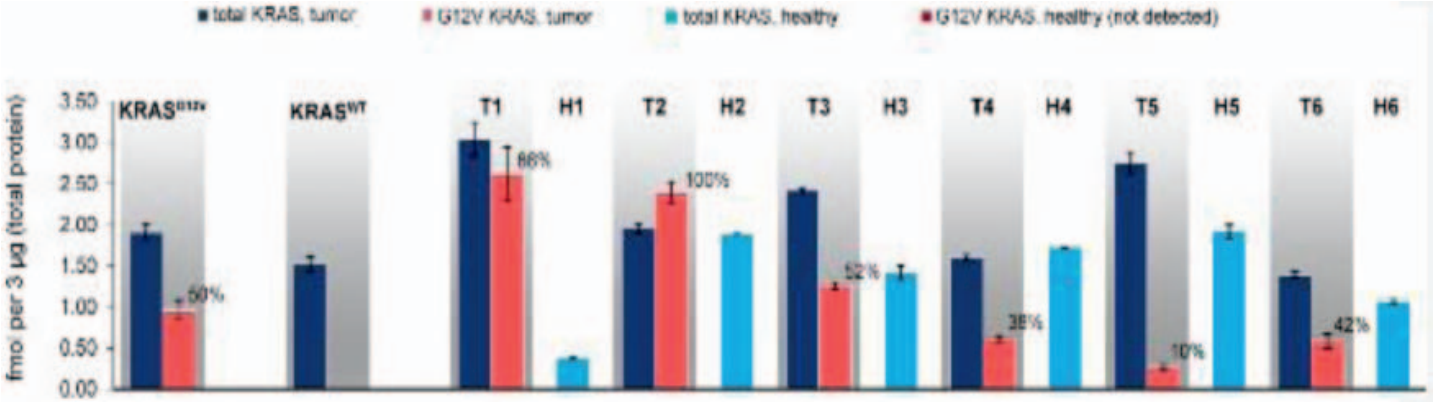

Abstract 1, Figure 1.

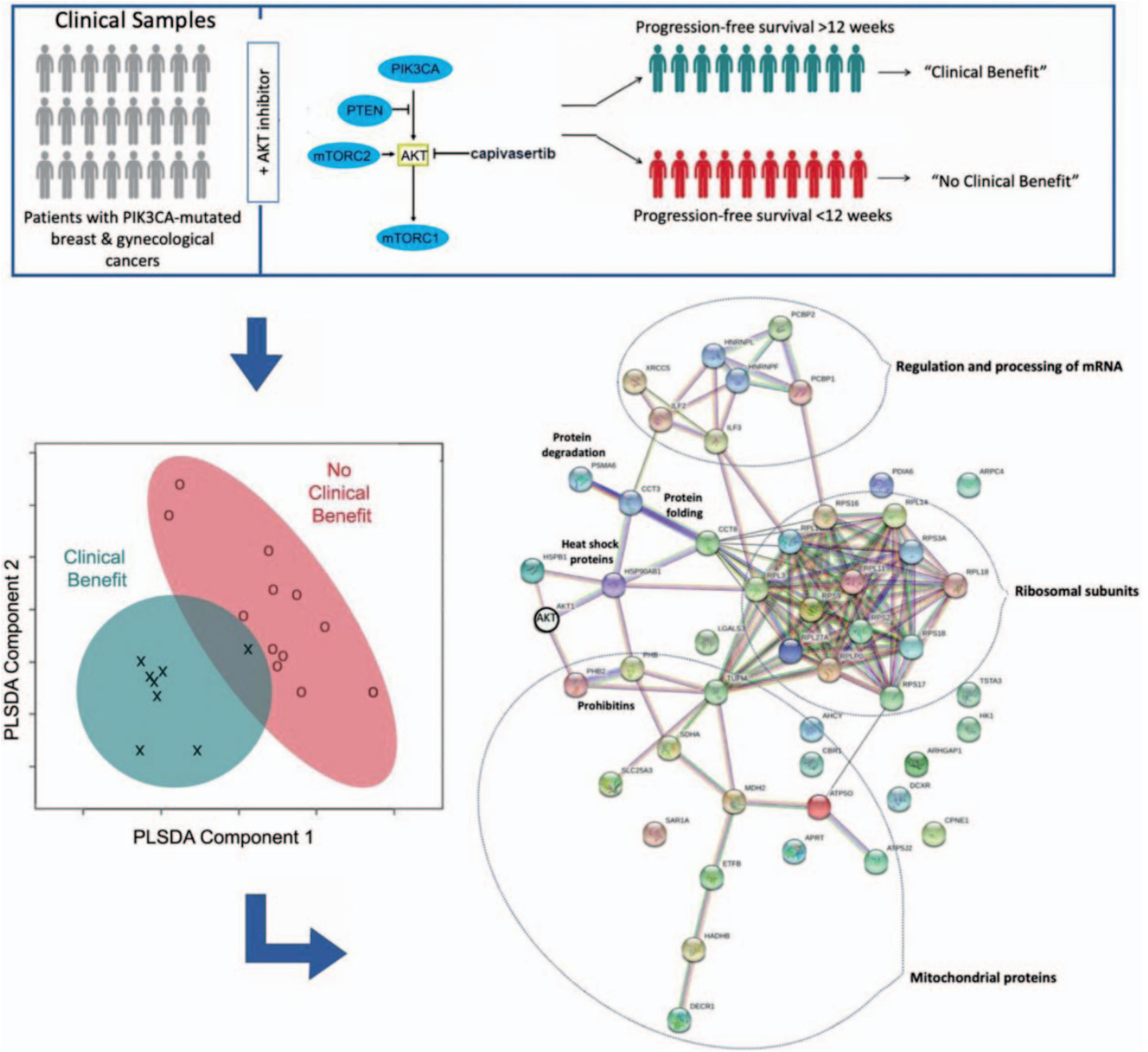

Abstract 1, Figure 2.

always predict downstream effects. Pre-clinical and clinical data show that protein levels can diverge from transcriptomic (mRNA). Here we present two examples (in colorectal cancer (CRC) and breast cancer) of the critical value of deep proteomic analysis to optimize the development of predictive biomarkers. Hotspot testing for activating *KRAS* mutations is used in precision oncology to select patients with CRC for anti-EGFR treatment. However, even for $KRAS^{WT}$ tumors anti-EGFR response rates are <30%, while mutated- *KRAS* does not entirely rule out response, indicating the need for improved patient stratification. Another example is the uncoupling of AKT activity from *PIK3CA* mutations in some cancers, where protein levels of typical markers of pathway activity, such as pAKT, pS6, and p4EBP1, are not always elevated in Luminal A breast cancers with activating *PIK3CA* mutations. **Methods:** We performed proteogenomic phenotyping of $KRAS^{wildtype}$ and $KRAS^{G12V}$ in CRC liver metastases (mCRC) obtained in a trial with serial biopsies. Among >9000 proteins we detected considerable expression changes including numerous proteins involved in progression and resistance in CRC. We identified peptides representing a number of predicted somatic mutations, including

$KRAS^{G12V}$. For eight of these, we developed a multiplexed parallel reaction monitoring (PRM) mass spectrometry assay to precisely quantify the mutated and canonical protein variants. To evaluate the utility of proteomics for predicting treatment response to the AKT inhibitor capivasertib in breast cancer, we utilized modern mass spectrometry-based methods to directly analyze the protein content of FFPE tumor tissues from patients. With a new serialized workflow, we acquired global proteomic data using nano-LC-MS/MS, followed raw global proteome data processing using Proteome DiscovererTM 2.4 and network and pathway analytic databases to define the global PI3K pathway proteomic status. **Results:** Proteomic phenotyping of eight mCRC tumors showed that total KRAS expression varied (0.47-1.01 fmol/μg total protein). In $KRAS^{G12V}$-mCRC, G12V-mutation levels were 42-100%, while one patient had only 10% $KRAS^{G12V}$ but 90% $KRAS^{WT}$. In breast cancer tissues, although the concentrations of the targeted protein (AKT) did not correlate with clinical outcome, global proteomics and network and pathway analysis point to greater upstream activation of AKT in the patients who did benefit, while resistant patients' tumors showed a profile of dysregulated protein biosynthesis (increased translation, mRNA processing, protein processing) and associated changes in energy balance (mitochondrial proteins). **Conclusion**: Analysis of metastatic lesions is critical to define the molecular profiles of the tumors being actually treated. Our proteomic analysis of KRAS status might represent a missed therapeutic opportunity: based on hotspot sequencing, the patient was excluded from anti- EGFR treatment, while PRM-based tumor-phenotyping indicates the patient might have benefitted from anti-EGFR therapy. Global proteomic profiling may help predict response to an AKT inhibitor, and may also suggest novel combinations for clinical testing.

Abstract No: 2

Clinically relevant chemotherapy modulates the tumor microenvironment and enhances immune cell killing of microsatellite stable and instable colorectal cancer cells

Lindsey Carlsen, Kelsey E. Huntington, Laura Wu, William MacDonald, Brooke Verschleiser, Wafik S. El-Deiry

Brown University, Providence, RI, USA

Introduction: Colorectal cancer (CRC) is the third most deadly cancer and has a 13% 5-year survival rate after metastasis. Most patients with metastatic CRC (mCRC) receive 5-FU + folinic acid combined with oxaliplatin, irinotecan, or both. Approximately 3% of patients with mCRC have tumors that are microsatellite instable (MSI), leading to high tumor infiltration of anti-tumor immune cells and sensitivity to immunotherapy. The other 97% of patients with mCRC have tumors that are microsatellite stable (MSS), immunologically "cold," and resistant to immunotherapy. Chemotherapy-mediated sensitization of MSS CRC tumors to immune cell killing has been described in preclinical models and in the CheckMate 9X8 trial, which suggests benefit of adding immunotherapy to chemotherapy for patients with consensus molecular subtype 3 tumors. We hypothesize that short-term (24 hour) pre-treatment of CRC cells with chemotherapy modulates the tumor microenvironment and enhances immune cell-mediated killing of CRC cells. **Methods:** HT29 (MSS) or HCT 116 (MSI) CRC cells were treated with clinically relevant chemotherapy combinations for 24 hours, then were co-cultured with TALL-104 or NK-92 cells for 4-24 hours to measure immune cell-mediated killing. The Luminex 200 platform was used to analyze a panel of 52 cytokines in the supernatant of HT29 and HCT 116 cells after treatment with clinically relevant chemotherapy combinations for 48 hours. A humanized mouse model was established by injecting HCT 116 tumor-bearing nude mice with TALL-104 cells. Infiltration of injected TALL-104 cells was measured in mice that received vehicle, 5-FU + oxaliplatin, or 5-FU + irinotecan. **Results**: TALL-104-mediated killing was significantly enhanced in HT29 cells pre-treated for 24 hours with 5-FU + irinotecan + oxaliplatin or 5-FU + folinic acid + oxaliplatin +/- pembrolizumab after 4 or 8 hours of co-culture. TALL-104- mediated killing was significantly enhanced in HCT 116 cells pre-treated with 5-FU + irinotecan + oxaliplatin after 4 or 24 hours of co-culture, and NK-92- mediated killing was enhanced after pre-treatment with 5-FU + oxaliplatin. In HT29 cells, all chemotherapy combinations tested (5-FU + oxaliplatin, 5-FU + irinotecan, and 5-FU + oxaliplatin + irinotecan) significantly increased GM-CSF and CXCL5 and decreased VEGF and CXCL10. Similar observations were made as far as GM-CSF and VEGF in HCT 116 cells treated with each of these combinations. Additionally, PD-L1, ferritin, CXCL14, TRAIL R2, and TRAIL R3 increased and IFN-β decreased in HCT 116 cells. In the HCT 116 + TALL-104 humanized mouse model, there was a trend toward increased TALL-104 cell infiltration in tumors of mice that were pre-treated with chemotherapy as compared to the control. **Conclusion:** Chemotherapy pre-treatment enhances immune cell killing of HT29 and HCT 116 cells as early as 24 hours after treatment. Addition of pembrolizumab does not suppress this effect in HT29 cells. PD-L1 upregulation may mediate this enhancement in HCT 116 cells but not in HT29 cells. Chemotherapy pre- treatment may enhance TALL-104 cell infiltration in MSI tumors. Further validation in MSS tumor models and optimization of chemotherapy + immunotherapy treatment strategies are needed in terms of dos, timing, and sequential versus concurrent treatment, as we are currently investigating. Validation and optimization of chemotherapy + immunotherapy treatment strategies could benefit a majority of patients with mCRC.

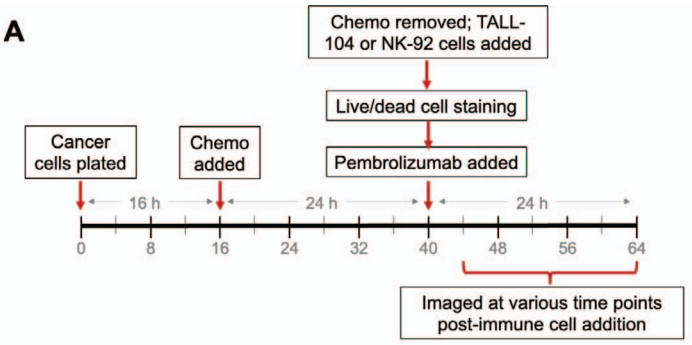

Figure 1. Pre-treatment of HT29 CRC cells with clinically relevant chemotherapy regimens enhances TALL-104-mediated killing. A) Experimental timeline. Cancer cells were treated with clinically relevant chemotherapy combinations for 24 hours, then chemotherapy was removed and TALL-104 or NK-92 cells were added at a 1:1 ratio with cancer cells +/- pembrolizumab. After 4-24 hours of co-culture, images were taken with a fluorescent microscope to quantify live cancer cells, live immune cells, and dead cells.

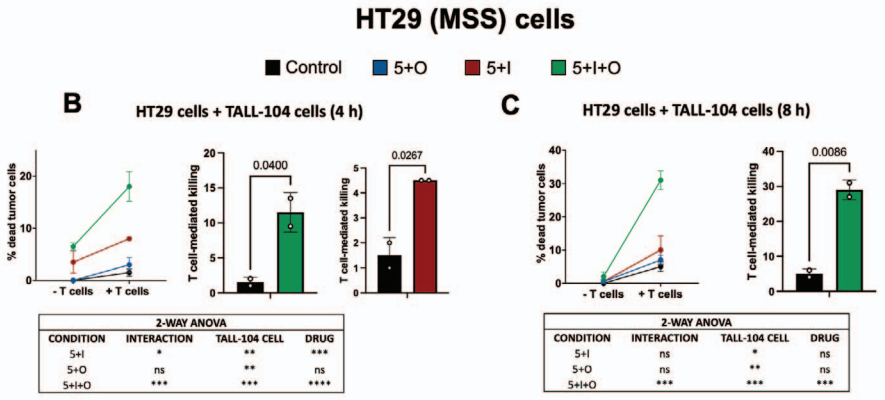

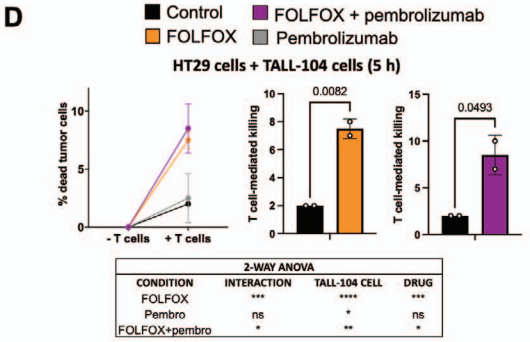

B) Normalized data indicating % dead tumor cells (left), corresponding two-way ANOVA to determine interaction effect between chemotherapy and immune cells (bottom), and normalized data indicating TALL-104-mediated cell killing (right) of HT29 cells pre-treated (24 hours) with chemotherapy followed by 4 hours of co-culture with TALL-104 cells. A significant interaction effect and significant enhancement of TALL-104-mediated killing was observed for HT29 cells that were pre-treated (24 hours) with 5+I+O and 5+I as compared to control, though the magnitude of this effect was larger for the 5+I+O group. **C)** A significant interaction effect and significant enhancement of TALL-104-mediated killing after 8 hours of co-culture was observed for HT29 cells that were pre-treated (24 hours) with 5+I+O as compared to control. **D)** A significant interaction effect and significant enhancement of TALL-104-mediated killing after 5 hours of co-culture was observed for HT29 cells that were pre-treated (24 hours) with FOLFOX and FOLFOX+pembrolizumab as compared to control. Pembrolizumab alone did not enhance TALL-104-mediated killing, in line with the weak expression of PD-L1 in HT29 cells. 5, 5-FU; I, irionotecan; O, oxaliplatin; FOLFOX, folonic acid + 5-FU + oxaliplatin.

Abstract 2, Figure 1.

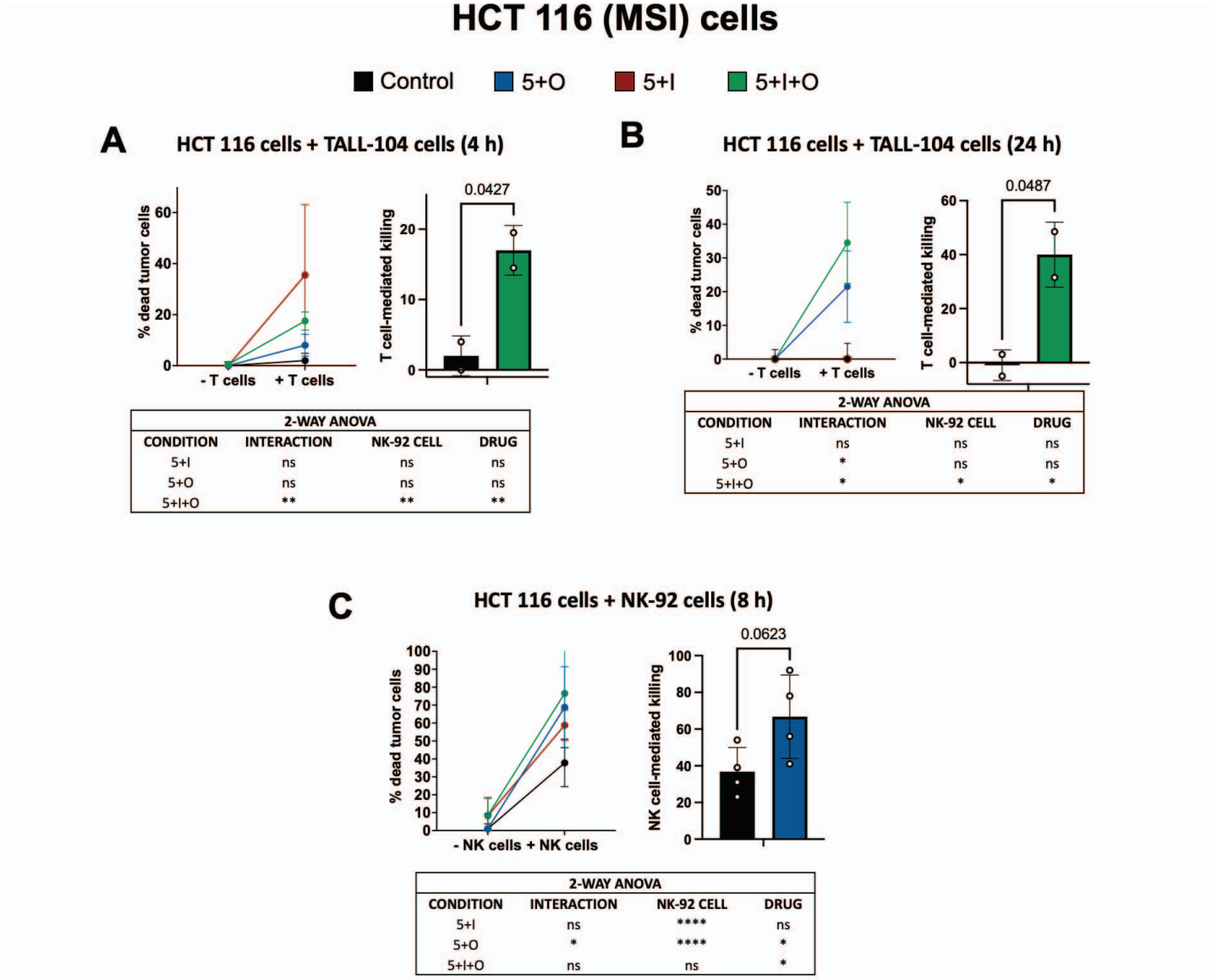

Figure 2. Pre-treatment of HCT 116 CRC cells with clinically relevant chemotherapy regimens enhances TALL-104-mediated killing and may enhance NK-92-mediated killing. A) Normalized data indicating % dead tumor cells (left), corresponding two-way ANOVA to determine interaction effect between chemotherapy and immune cells (bottom), and normalized data indicating TALL-104-mediated cell killing (right) of HCT 116 cells pre-treated (24 hours) with chemotherapy followed by 4 hours of co-culture with TALL-104 cells. Same experimental timeline shown in Figure 1A was used. A significant interaction effect and significant enhancement of TALL-104-mediated killing after 4 hours of co-culture was observed for HCT 116 cells that were pre-treated (24 hours) with 5+I+O as compared to control. B) A significant interaction effect and significant enhancement of TALL-104-mediated killing after 24 hours of co-culture was observed for HCT 116 cells that were pre-treated (24 hours) with 5+I+O as compared to control. C) A significant interaction effect and nearly significant enhancement of NK-92-mediated killing after 8 hours of co-culture was observed for HCT 116 cells that were pre-treated (24 hours) with 5+O as compared to control. 5, 5-FU; I, irionotecan; O, oxaliplatin; FOLFOX, folonic acid + 5-FU + oxaliplatin.

Abstract 2, Figure 2.

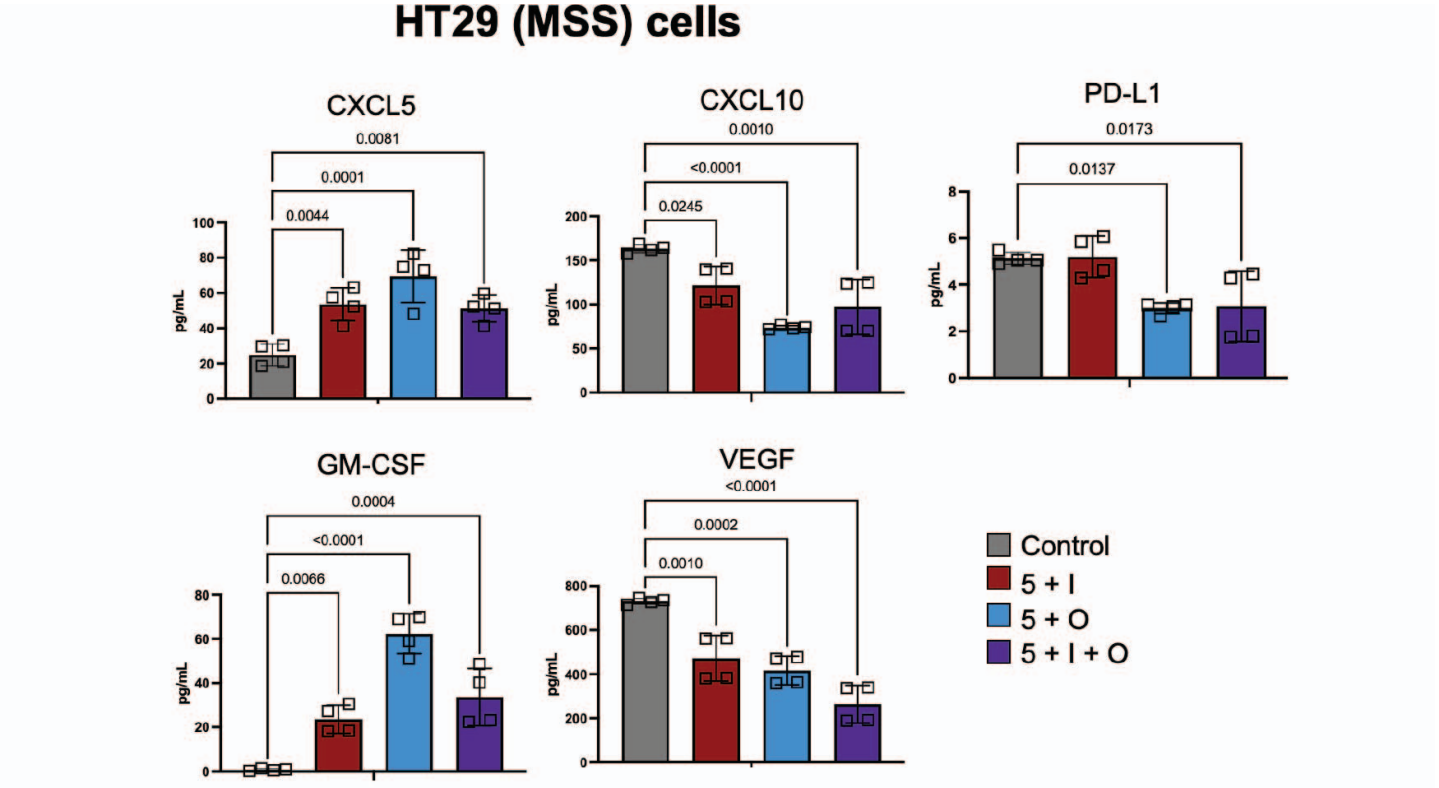

Figure 3. Treatment of HT29 CRC cells with clinically relevant chemotherapy regimens for 48 hours modulates cytokine secretion. An increase in secretion of GM-CSF and CXCL5 was noted, while CXCL10 and VEGF secretion was suppressed. PD-L1, an important predictive biomarker for immunotherapy, may be slightly decreased or remain constant after chemotherapy treatment of HT29 cells. p-values calculated by one-way ANOVA. 5, 5-FU; I, irionotecan; O, oxaliplatin; FOLFOX, folonic acid + 5-FU + oxaliplatin.

Abstract 2, Figure 3.

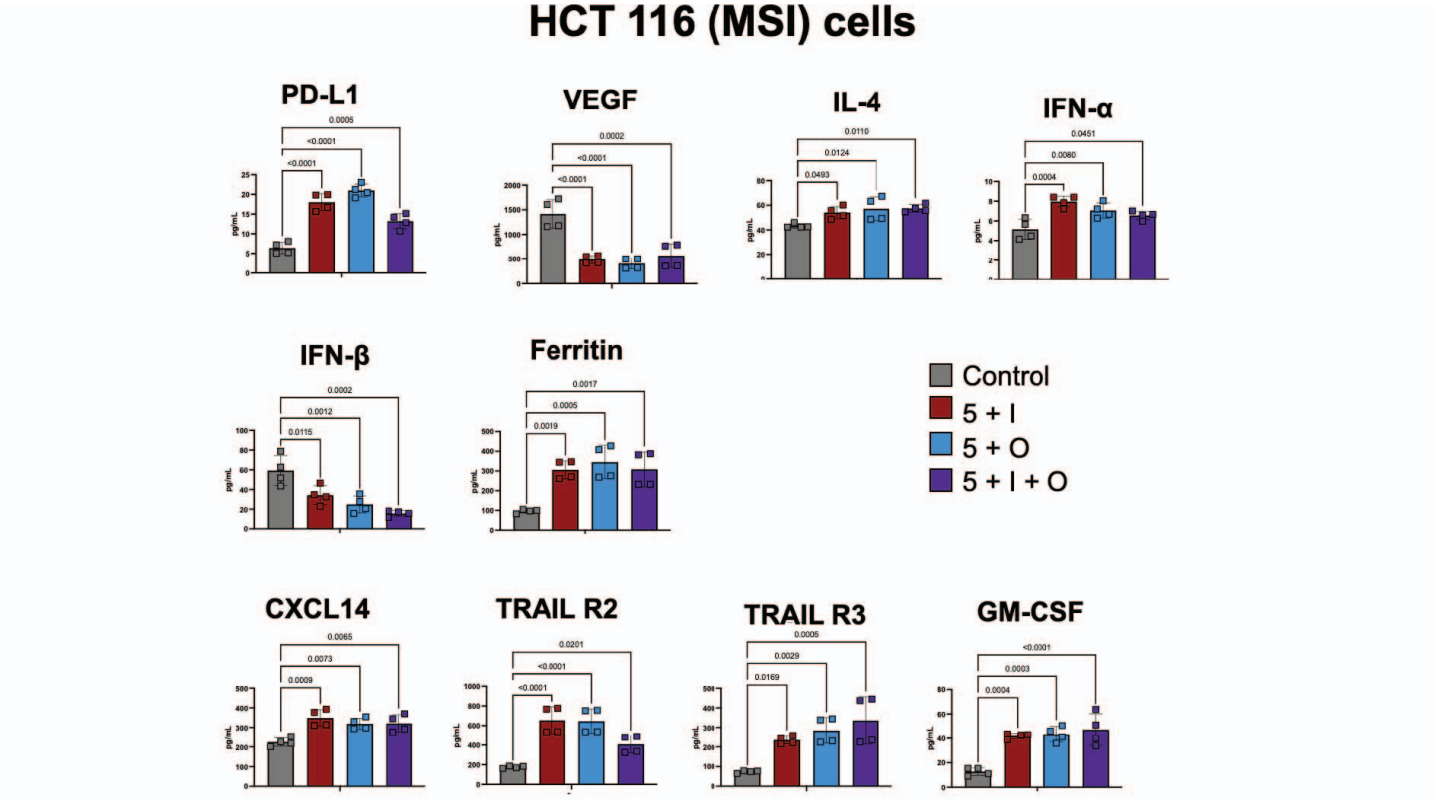

Figure 4. Treatment of HCT 116 CRC cells with clinically relevant chemotherapy regimens for 48 hours modulates cytokine secretion. A significant increase in secretion was noted for GM-CSF, PD-L1, ferritin, CXCL14, TRAIL R2, and TRAIL R3. A smaller magnitude but still statistically significant increase was noted for IFN-α and IL-4. A decrease in secretion was noted for IFN-β and VEGF. p-values calculated by one-way ANOVA. 5, 5-FU; I, irionotecan; O, oxaliplatin; FOLFOX, folonic acid + 5-FU + oxaliplatin.

Abstract 2, Figure 4.

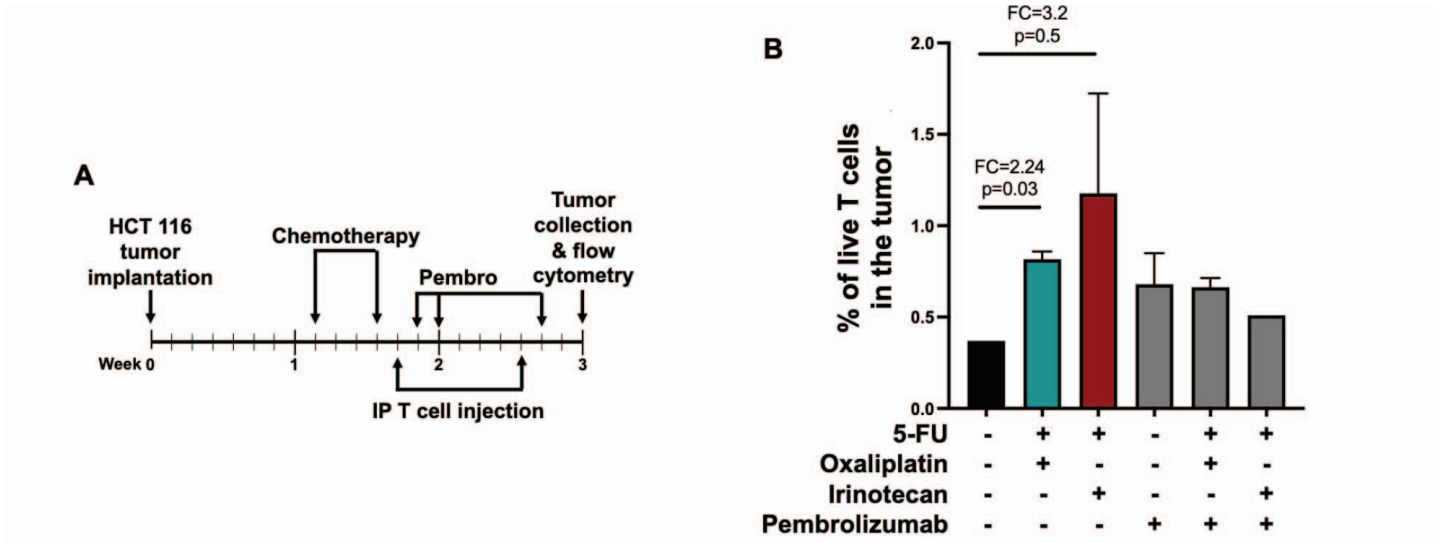

Figure 5. Chemotherapy treatment two days before pembrolizumab treatment enhances infiltration of TALL-104 cells into HCT 116 tumors. A) Experimental timeline. Following HCT 116 tumor implantation, mice were given two doses of either 5-FU+oxaliplatin or 5-FU+irinotecan. Mice then received alternating injections of TALL-104 cells and pembrolizumab for one week, then were sacrificed for analysis of TALL-104 cell infiltration into the tumor by flow cytometry. B) 5-FU+oxaliplatin and 5-FU+irinotecan treatment may enhance infiltration of TALL-104 cells into the tumor. This effect was not enhanced or suppressed by addition of pembrolizumab. FC, fold change.

Abstract 2, Figure 5.

Abstract No: 3

Bridging morphology, molecular pathology, bioinformatics, and cancer genomics to discover better early-stage lung cancer biomarkers

Paul Chiroi[1], Radu Pirlog[1], Ioana Rusu[2], Ancuta Jurj[1], Liviuta Budisan[1], Cecilia Bica[1], Cornelia Braicu[1], Doinita Crisan[3], Ioana Berindan-Neagoe[1]

[1]Research Center for Functional Genomics, Biomedicine and Translational Medicine, Iuliu Hatieganu University of Medicine and Pharmacy, Cluj-Napoca, Romania
[2]Regional Institute of Gastroenterology and Hepatology, Cluj-Napoca, Romania; Iuliu Hatieganu University of Medicine and Pharmacy, Cluj-Napoca, Romania
[3]Department of Morphological Sciences, Iuliu Hatieganu University of Medicine and Pharmacy, Cluj-Napoca, Romania

Introduction: Lung cancer (LC) is the largest cause of cancer-related death worldwide, accounting for over 1,8 million deaths each year. Despite all technological advancements made so far, 57% of patients are diagnosed in late stages. Hence, the central focus of our study was understanding the alterations in lung morphology, tumor microenvironment (TME) and genomic landscape of LC, to unlock a new avenue for discovering novel, early-stage biomarkers. **Methods:** A cohort of 51 patients with early-stage LC were diagnosed between January 2013-December 2016. Histological diagnosis and staging were done according to standard protocols. Immunohistochemistry staining was used for E-cadherin, p53, CD4, and CD8. Tumor zones with more than 15% tumor cells were marked for further isolation and molecular analysis. Total RNA was extracted from FFPE tissues using Qiagen RNeasy FFPE Kit. We used miRNET to identify miRNAs that could be used as biomarkers for early-stage diagnosis. The synthesis of cDNA was performed using 100 ng of total RNA. The qRT-PCR data analysis was done using ΔΔCt method. Based on IHC markers and early-stage LC clinical biomarkers we generated a network of interactions between miRNAs and their target genes. **Results:** Histology results divided our patient cohort in 43.1% lung adenocarcinomas, 41.1% lung squamous cell carcinomas and 15.8% neuroendocrine lung tumors. The pathological stages included 47.1% stage IA, 37.2% IB and 15.7% of IIA cases. E-cadherin IHC was intensely positive in 19 cases and moderately positive in 32 cases. P53 IHC was positive in 23 cases and negative in 28 cases. TME analysis showed a moderate to high peritumoral inflammatory infiltrate in 80% of the cases. Differential expression analysis of the selected miRNAs revealed a statistically significant down-regulation of hsa-miR-29b-3p and hsa-miR-181a-5p in tumor tissue, while hsa-miR-205-5p and hsa-miR-25-3p were upregulated in LC tumor tissue when compared with adjacent controls.

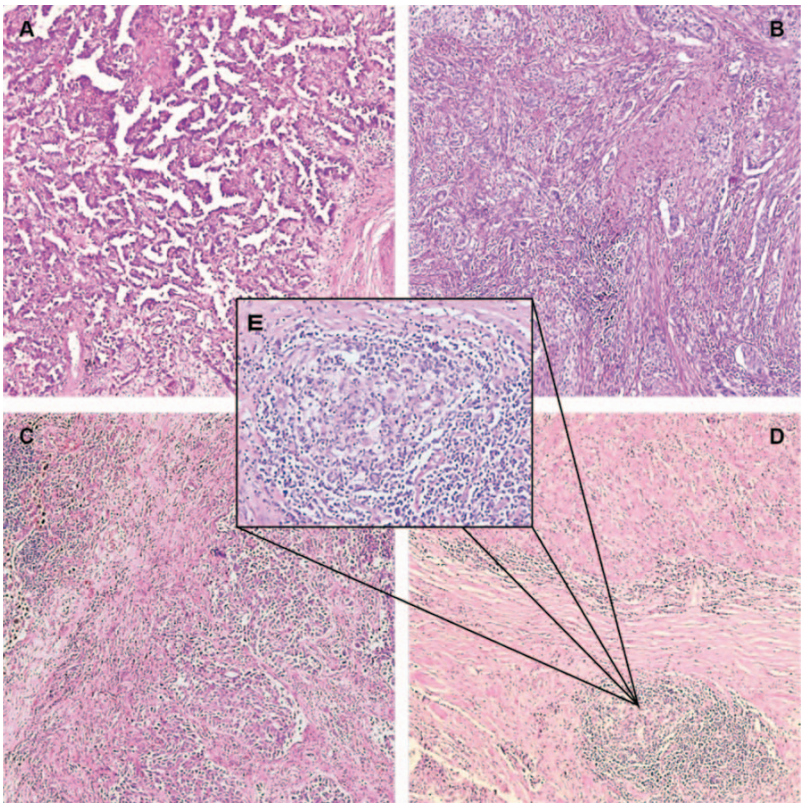

Abstract 3, Figure 1.

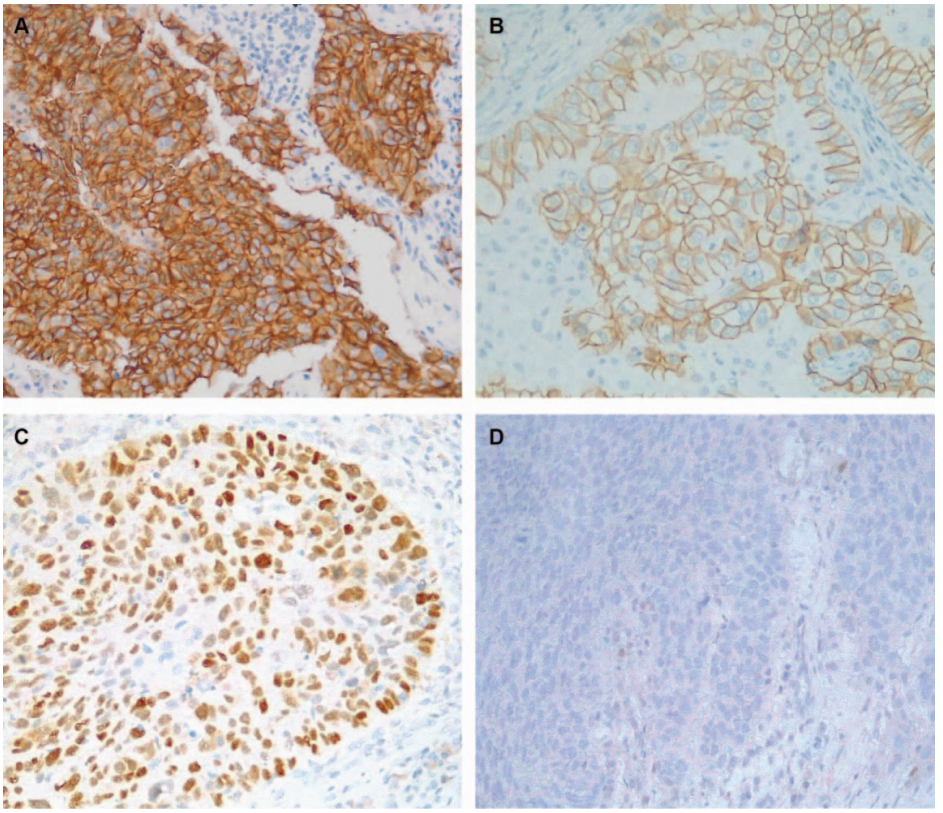

Abstract 3, Figure 2. A: E-cadherin 3+; B: E-cadherin 2+; C: p53 positive; D: p53 negative.

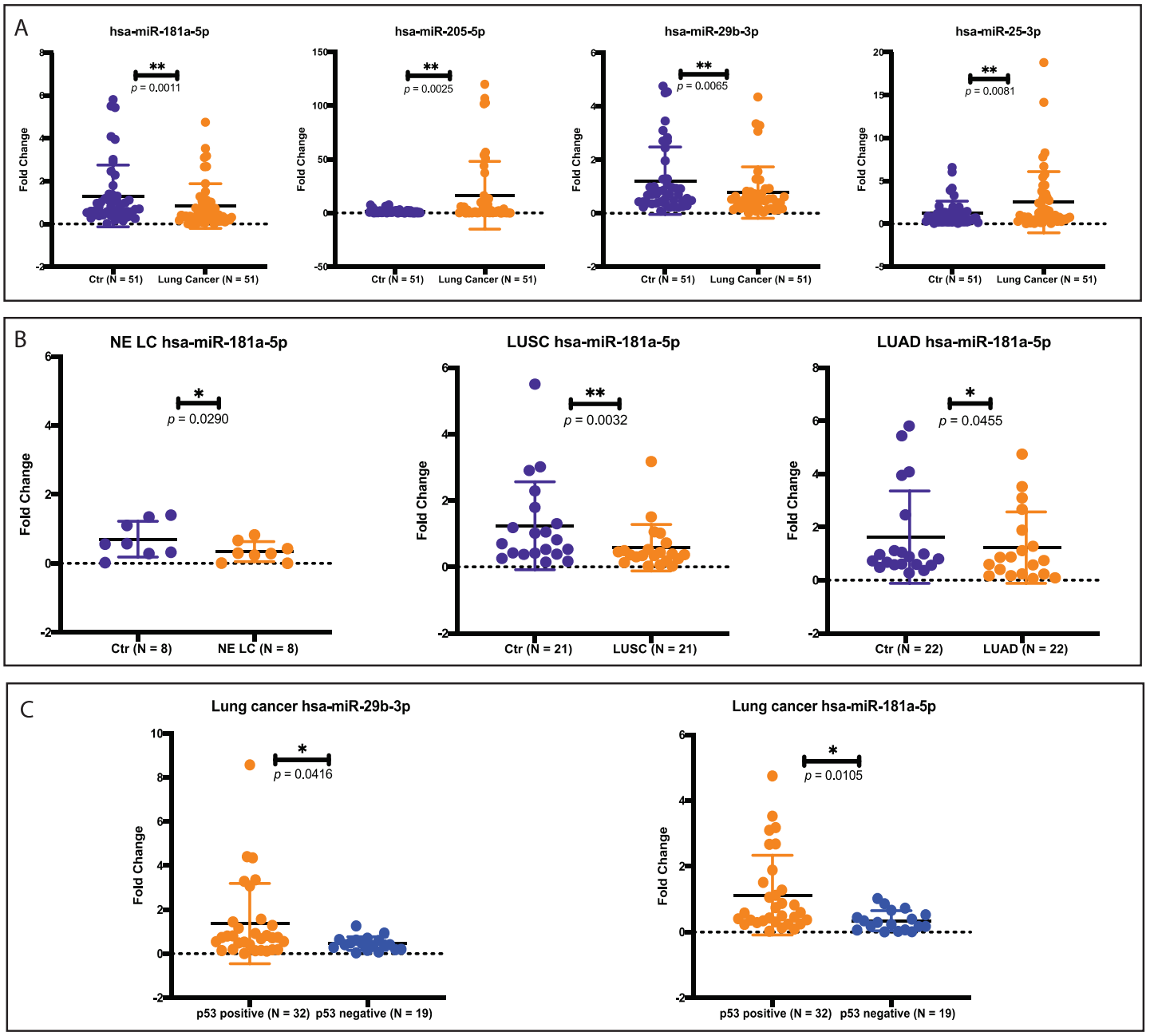

Abstract 3, Figure 3.

Conclusion: Our study is an in-depth characterization of TME in a subset of early-stage LC that includes both NSCLC and SCLC. These tumors are immunologic active with an 80% moderate to high inflammatory TME, as most inflammatory infiltrate is localized in the stromal compartment where TLS were present in 74,5% of the cases. The main component of the TME were CD4 cells. Based on the bioinformatic analysis we managed to validate 4 miRNAs (hsa-miR-29b-3p, hsa-miR-181a-5p, hsa-miR-205-5p, hsa-miR-25-3p) that were dysregulated in the tumoral tissue compared with the adjacent normal zones, and that could be further investigated as potential biomarkers for early-stage LC. Approaching such a heterogeneous disease as LC from multiple angles including morphology, molecular pathology, bioinformatics, and cancer genomics allows us to assemble different pieces of the same puzzle in the quest for novel, early-stage biomarker identification.

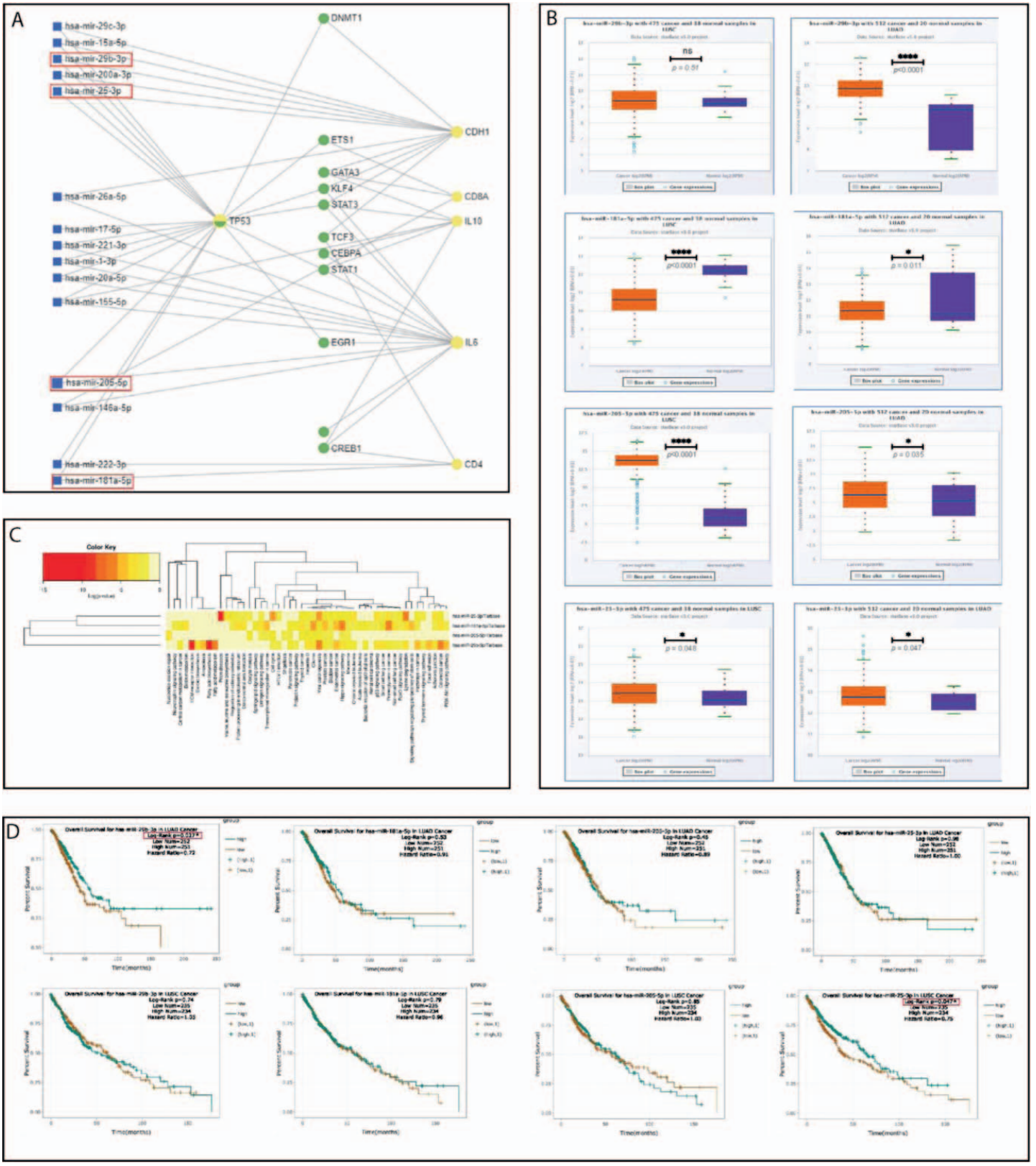

Abstract 3, Figure 4.

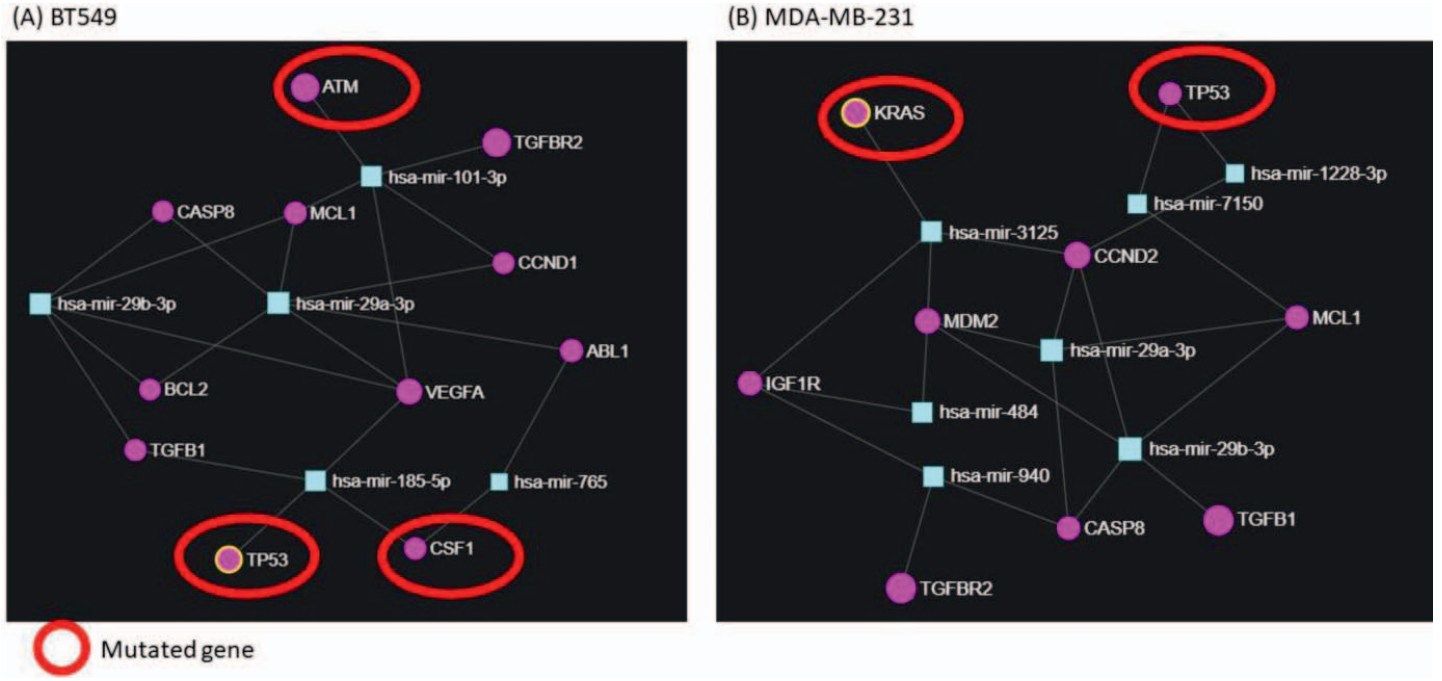

Abstract 4, Figure 1. A complex regulatory signaling mechanism related to miR-29 inhibition, emphasis interconnection of the altered miRNA with specific mutated genes in both TNBC cell lines. The network interaction between mRNA-miRNA generated by using miRNet software. (A) The main mutated genes, *ATM*, *TP53* and *CSF1*, found in BT549 cell line as an established interaction between miR-29a-3p and miR-29b-3p. (B) The main mutated genes, *KRAS* and *TP53*, found in MDA-MB-231 cell line as an established interaction between miR-29a-3p and miR-29b-3p (mutated genes are highlighted in red circles).

Abstract No: 4

Exploring the potential of miR-29b as a therapeutic for triple negative breast cancer

Cornelia Braicu[1], Ancuta Jurj[1], Oana Zanoaga[1], Lajos Raduly[1], Vlad Morhan[1,2], Zsofi Papi[3], Cristina Ciocan[1], Laura Pop[1], Ioana Berindan-Neagoe[1]

[1]Research Center for Functional Genomics, Biomedicine and Translational Medicine, The Iuliu Hatieganu University of Medicine and Pharmacy, Cluj-Napoca, Romania
[2]Faculty of Medicine- The Iuliu Hatieganu University of Medicine and Pharmacy, Cluj- Napoca, Romania
[3]Faculty of Medicine, University of Szeged, Szeged, Hungary

Introduction: Lacking specific therapies triple negative breast cancer (TNBC) has a limited clinical outcome and poor survival. MiRNAs are newly proposed as potential therapeutics in cancer; miR-29b gained a particular attention and we evaluate the therapeutic potential in TNBC in vitro studies. **Methods**: Functional assays and miRNAs microarray were done using transient transfection protocol for miR-29b inhibitor and negative control (50 nM). **Results**: MiR-29b in TCGA cohort is upregulated and corelated with overall survival. MiR-29b inhibition was associated with a reduced cell proliferation, apoptosis and autophagy; an altered miRNA pattern was observed (BT549:11-down and 8-up and MDA-MB- 231: 33-down and 10-up). Common miRNA signature was represented by miR-29a/b and miR-1229. Using DIANA-miRPath, targeted genes were linked to extracellular matrix and TP53 signaling; *MCL1* and *TGFB1* were validated by qRT-PCR. **Conclusion**: miR-29b inhibited cell proliferation through the activation of apoptosis and autophagy, presenting a complex regulatory mechanism.

Abstract No: 5

Whole genome sequencing-based cancer diagnostics for precision medicine in routine practice

Edwin Cuppen[1], Hans van Snellenberg[1], Gerrit Meijer[2], Kim Monkhorst[2]

[1]Hartwig Medical Foundation, Amsterdam, Netherlands
[2]Netherlands Cancer Institute, Amsterdam, Netherlands

Introduction: The current surge in number and diversity of targeted anti-cancer agents poses increasing challenges to molecular cancer diagnostics, resulting in underdiagnosis and undertreatment. Whole genome sequencing (WGS) is maturing rapidly as a powerful diagnostic technique and may provide a sustainable solution for addressing today's as well as future diagnostic challenges**. Methods:** I will present technical analysis details underlying the routine ISO-accredited workflow that we implemented and which is now used to support multiple hospitals in the Netherlands for

routine WGS-based cancer diagnostics with turnaround times of less than 10 days from 'biopsy' in to 'patient report with therapy guidance' out. I will also share details from a prospective study on the feasibility, validity and value of WGS in routine pathology practice based on a direct comparison with standard of care diagnostics for 1200 patients. **Results:** We found >99% concordance with SOC, but WGS identified additional actionable biomarkers in 60-70% of cases with >25% of patients starting biomarker-based therapy in regular or clinical trial setting based on these extra findings. Finally, utility of WGS, but also the importance of databases with genomic and clinical data, for patients with cancer of unknown primary will be highlighted. **Conclusion:** Whole genome sequencing is a valid and feasible diagnostic tool for diagnostics in oncology with added value for selected patients with cancer. This project has led to the implementation of WGS in routine diagnostics a comprehensive cancer center.

Abstract No: 7

Neoadjuvant carboplatin in triple-negative breast cancer: results from the NaCaTRINE trial, a phase II single study.

Ana Cecília de Oliveira Lessa[1], Ana Suellen Barroso Carneiro[1], Domício Carvalho Lacerda[1], Carlos Eduardo Paiva[1], Marina Moreira Costa Zorzetto[1], Antônio Bailão Junior[1], Idam de Oliveira Junior[1], Ana Julia Aguiar de Freitas[2], Amanda Aparecida Splendor Solera[2], Edenir Inêz Palmero[2], Márcia Maria Chiquitelli Marques[2], Cristiano de Pádua Souza[1]

[1]Barretos Cancer Hospital, Barretos, São Paulo, Brazil
[2]Molecular Oncology Research Center, Barretos Cancer Hospital, Teaching and Research Institute, Barretos, São Paulo, Brazil

Introduction: Triple-negative Breast Cancer (TNBC) is a heterogeneous disease with high risk of recurrence, even for early stages. Although TNBC is characterized by aggressive behavior, it is sensitive to cytotoxity agents. Carboplatin is a cytotoxic DNA damaging agent to leading to DNA strand breaks and consecutive cell apoptosis which could enhance anthracycline and taxanes effects in neoadjuvant treatment. We aimed to assess the efficacy of the addition of carboplatin to neoadjuvant anthracycline and taxanes for TNBC. **Method:** NaCaTRINe was a phase II, single center, open label, randomized trial. Women untreated TNBC, unilateral or bilateral, were enrolled into our study if they provided written informed consent. TNBC status was defined as estrogen and progesterone receptor levels less than 1% and HER2 negative. Patients were eligible if older than 18 years, with performance status ≤ 1, clinical stage T1N1-3 or T2-T4d and N0-N3. All eligible patients were randomized in 1:1 ratio to Carboplatin group: doxorubicin (60 mg/m2) plus cyclophosphamide (600 mg/m2) both intravenously (IV) once every 21 days for four cycles followed by paclitaxel (80 mg/m2 IV) once every 7 days for twelve cycles with carboplatin AUC 1.5 (experimental arm) once every 7 days for twelve cycles or without carboplatin (control arm). Randomization was stratified according to *gBRCA* status (deleterious mutation vs no deleterious mutations), age (< 50 vs ≥ 50 years) or AJCC 8th clinical stage (II vs III). N0 was defined as negative imaging, no clinical palpation or suspicious imaging without a cytological confirmation. The primary endpoint was pathological complete responses (pCR) rate. pCR was defined as no invasive tumor in the breast and lymph nodes (ypT0ypN0). Secondary endpoints were recurrence-free survival (RFS) and overall survival (OS). This trial is registered with ClinicalTrials.gov Identifier: NCT02978495. **Results:** Between Mar 29, 2017 and Mar 24, 2021, we screened 154 patients at a single site in Brazil for eligibility and randomized 146 patients (73 in Carboplatin containing regimen and 73 in Non-Carboplatin containing regimen). The pCR rate (ypT0ypN0) was 43.8% (32 of 73 patients) in the Carboplatin containing regimen and 30.1% (22 of 73 patients) in the Non-Carboplatin containing regimen not meeting the prespecified goal of increase the pCR in 15% (*P* value = 0.304). Pathogenic BRCA mutations were present in 29 (19.8%) of 146 cases. The pCR rate was 18 (62%) of 29 in patients with pathogenic BRCA mutations. In the Carboplatin arm, 11 (61.1%) of 15 patients with BRCA mutation achieved a pCR, compared with 21 (36.2%) of 58 patients without BRCA mutations. In the Non-Carboplatin arm, 7 (50%) of 14 patients with BRCA mutation achieved a pCR, compared with 15 (25.4%) of 59 patients without BRCA mutations. The median of RFS was not reached. At 3 years, the proportion of patients without recurrence was 66% in the Carboplatin containing regimen and 69.6% in the Non-Carboplatin containing regimen, and the proportion of patients alive was 71.6% in the Carboplatin containing regimen and 75.5% in the Non-Carboplatin containing regimen. **Conclusion:** The addition of neoadjuvant carboplatin to a regimen of anthracycline and taxane did not increase significantly the proportion of patients achieving pathological complete response, RFS and OS.

Abstract No: 8

Clinical features of patients with MTAP-mutated advanced bladder cancer

Andre De Souza [1,2], Anthony Mega[1,2], John Douglass [1], Dragan Golijanin[4], Amin Ali [3], Adam Olszewski [1,2], Alper Uzun, Ece D Gamsiz Uzun, Sheldon Holder [1,2], Galina Lagos [1,2], Howard Safran[1,2], Wafik S El-Deiry [1,2,3], Benedito A Carneiro[1,2]

[1]*Hematology-Oncology Division, Department of Medicine, Brown University, Providence, RI, USA*
[2]*Legorreta Cancer Center at Brown University, The Warren Alpert Medical School, Brown University, Providence, RI, USA*
[3]*Department of Pathology and Laboratory Medicine, The Warren Alpert Medical School, Brown University, Providence, RI, USA*
[4]*Department of Urology, Brown University, Providence, RI, USA*

Introduction: Patients with advanced urothelial carcinoma have a dismal prognosis despite several new therapies available in the clinic in the last 5 years. FGFR2 fusions, FGFR3 mutations and fusions, PD-L1 expression, tumor mutational burden, and microsatellite instability are established predictive biomarkers in advanced urothelial carcinoma. Novel biomarkers can optimize the sequencing of available treatments and improve outcomes. We describe herein clinical and pathologic features of patients with an aggressive subtype of bladder cancer characterized by deletion of the gene *MTAP* encoding the enzyme S-Methyl-5′- thioadenosine phosphatase, a potential biomarker of response to chemotherapy. **Methods**: Retrospective analysis of 61 patients with advanced urothelial carcinoma for whom demographics, pathologic specimens, next generation sequencing, and clinical outcomes were available. We compared the frequency of histology variants, upper tract location, pathogenic gene variants, tumor response, progression free survival (PFS) and overall survival (OS) between patients with tumors harboring MTAP deletion (MTAP-del) and wild type tumors (MTAP-WT). **Results:** MTAP-del occurred in 19 patients (31%). Tumors with MTAP-del were characterized by higher prevalence of squamous differentiation (47.4 vs 11.9%, P= 0.006498), bone metastases (52.6 vs 23.5%, P=0.018) and lower frequency of upper urinary tract location (5.2% vs 26.1%, P=0.087669). Alterations in the PIK3 and MAPK pathways were more frequent when MTAP was deleted. There was a trend to inferior response to chemotherapy among MTAP-del tumors, but no difference in the response to immune checkpoint inhibitors (46% vs 8%, P=0.6762) or enfortumab (33.3 % vs 42.8%, P=0.3420) between MTAP- del and MTAP-WT. Median progression free survival after first line therapy (PFS1) was 5.5 months for patients with MTAP-WT and 4.5 months in for patients with MTAP-del (HR= 1.30 (95%CI, 0.64-2.63), P= 0.471). Median OS from diagnosis of localized or de novo metastatic disease was 16 months (range 1.5- 60, IQR 8-26) for patients with MTAP-del and 24.5 months (range 3-156, IQR 16-48) for patients with MTAP-WT (P=0.0218) with no difference from the diagnosis of metastatic disease to death (P= 0.6346), suggesting that time to progression to metastatic disease is shorter in patients with MTAP-del. **Conclusions**: MTAP deletion occurs in 31% of patients with advanced urothelial carcinoma and defines a subgroup of patients with aggressive features, such as squamous differentiation, frequent bone metastases, poor response to chemotherapy and shorter time to progression to metastatic disease. Gene set enrichment pathway, in silico protein-to-protein interaction and other exploratory analyses are ongoing.

Abstract No: 9

Novel germline codon 72 p53 allele in a patient with AML, a strong family history of multiple cancers in the women, and mixing with FANCC and other alleles

Wafik El-Deiry

Legorreta Cancer Center at Brown University, Providence, RI, USA

Introduction: Patients with germ-line mutations in the p53 tumor suppressor gene are susceptible to develop various tumors at a young age as part of the Li-Fraumeni Syndrome. An inversion 16 acute myelogenous leukemia recurred in a patient and was treated with a bone marrow transplant. The patient presented to the clinic of the author who is an expert on p53 to understand why her family has multiple cancers and to understand the role of a p53 alteration that has not been reported in the germline and that was scored as a variant of unknown significance. **Methods**: Patient and family history were recorded. Reports of germline testing were reviewed. A pedigree was drafted. Leaders in the field of tumor suppressor genes, genomics, variants, were consulted and the case was also briefly discussed with additional leaders of the p53 field. The patient and her mother gave permission for her case to be discussed with others and for reports to be published as appropriate. The patient has discussed her medical history in recorded videos that are publicly available. **Results:** The patient is a 34-year-old woman with a history of brain arachnoid cysts and hydrocephalus requiring multiple interventions who developed leukemia that relapsed and has been in remission after bone marrow transplant. There is a novel allele in p53 at codon 72 that has not been reported in the germline and that was scored as a variant of unknown significance. Several family members carry pathogenic FANC alleles and don't have the p53 alteration, while the patient has the p53 allele and not the FANC allele. Interesting features in the family include a mixing of alleles among individuals who have developed cancer. The patient harbors the germ-line p53 alteration, while another family member developed breast cancer only has the FANC alleles. The patient's mother harbors the p53 Allele as well as a FANC allele and she developed basal cell skin cancer. The patient's maternal grandmother also harbored the p53 allele as well as the FANC allele. Other members in multiple generations have developed Ewing's Sarcoma, brain cancer, Hodgkin's disease, CLL, lung cancer, basal cell skin cancer and melanoma. To date the individuals in the family affected by cancer have all been females. **Conclusion:** The patient may be part of a Li-Fraumeni family with a novel mutation at codon 72. The mixing of pathogenic FANC alleles is somewhat unusual

and the occurrence of cancer among female members of the extended family is unexplained. Ongoing work includes functional analysis of the p53 alteration, and future plans to model the mixing of p53 and FANC alleles. A goal as we develop and translate therapeutics targeting tumors with loss-of-function or gain-of-function mutations in p53 is explore strategies for cancer prevention for example in Li-Fraumeni Syndrome affected individuals.

Abstract No: 10

Exceptional response to dual PARP and PIK3CA inhibition (PIK3i) in a patient with metastatic castration-resistant prostate cancer (mCRPC) harbouring *PALB2* and *PIK3CA* germline variants of undetermined significance (VUS)

Matthew Hadfield, André De Souza, Anthony Mega, Lauren Massingham, Dragan Golijanin, Lanlan Zhou, Kelsey Huntington, Wafik S El-Deiry, Benedito A Carneiro

Legorreta Cancer Center at Brown University, The Warren Alpert Medical School, Brown University, Providence, RI, USA

Introduction: Patients with mCRPC harboring DNA Double-strand Repair (DDR) gene alterations are sensitive to PARP inhibitors (PARPi). Preclinical and clinical data have demonstrated that PIK3CA inhibitors sensitize cancer cells to PARPi, even in the absence of DDR or PIK3CA mutations. PI3Ki compromises nucleoside synthesis and limits the nucleotide pool required for DDR. In addition, PARPi upregulates the PIK3 pathway. The combination of PIK3i and PARPi has emerged as a promising therapeutic strategy in prostate cancer. Among DDR gene alterations used to select for PARPi, pathogenic *PALB2* alterations are one the strongest predictive biomarkers. DDR VUS are frequently not considered in treatment decisions for PARPi. We present a patient with mCRPC with *PALB2* and *PIK3CA* VUS treated with PI3Ki and PARPi. **Methods**: Patient enrolled in the ongoing Brown University Oncology Group trial (BrUOG360) phase Ib/II study investigating safety and initial efficacy of the combination of an alpha and delta PI3KCA inhibitor (copanlisib) and a PARPi (rucaparib) in patients with previously treated mCRPC (NCT04253262). **Results:** A 52-year-old male (ECOG of 1) presented with lower urinary tract symptoms in June 2018 and elevated PSA. Prostate biopsy revealed Gleason 4+4=8 in 9 out of 12 cores. Bone scan showed multiple osteoblastic sites of disease and MRI of the pelvis showed pathologic pelvic adenopathy. NGS of prostate tumor specimen showed somatic alteration in *TP53* (c.883C>G) and *UGCG* c.926A VUS and TMPRSS2-ERG translocation. Germline saliva-based testing showed germline VUS in *PALB2* (c.298 C>T (p.Leu100Phe) and *PIK3CA* (c.483T>C (silent). Patient was initially treated with androgen-deprivation therapy and after development of castration-resistance, he received androgen deprivation therapy, abiraterone, enzalutamide, docetaxel and cabazitaxel. The patient was then enrolled on a phase Ib/II evaluating the combination of copanlisib and rucaparib. The patient had prolonged PSA response, stable disease per RECIST, and marked clinical improvement lasting 18 months when he discontinued treatment due to progressive disease. Another tumor specimen submitted to NGS obtained upon progression showed the following new alterations suggestive of clonal evolution and possibly contributing to tumor resistance: *RAD51C* and PTEN copy number loss, *PIK3CA* (c.1986-2A>G), *SMAD4* (p.CY363Y), *MYC* copy number gain and other VUS in *EWSR1, SYNE1, PIK3CD, CBR3, MSH6, and EZH2*. **Conclusion**: This case highlights the potential benefit of the PIK3CA/PARPi combination for patients with prostate cancer harboring PALB2 (298C>T (p.Leu100Phe) and PIK3CA VUS. The functional impact of this PALB2 alteration in DNA repair mechanism warrants further investigation as it could be associated with sensitivity to PARPi. Multiple new alterations detected at progression could inform new resistance mechanisms. Ongoing studies will investigate the impact of this treatment in peripheral blood cytokine profile and further characterization of tumor microenvironment on tumor specimens obtained during the treatment.

Abstract No: 11

LITOseek Data platform, next generation Pan cancer immunotherapy response prediction

Sahar Hosseinian Ehrensberger[1], Victoria Wosika[1], Noushin Hadadi[1], Eric Durandau[1], Laura Ciarloni[1], Sylvain Monnier-Benoit[1], Paolo Angelino[2], Niven Mehra[3], Stefan Scherer[1]

[1]Novigenix SA, Switzerland
[2]SIB
[3]Radboud UMC

Introduction: While immune checkpoint inhibitors (ICI) have provided life-saving alternative treatment to number of metastatic patients, a significant percentage of patients do not achieve a clinical benefit. For metastatic melanoma (MM), the response rate is 40-60%, while it decreases to only 15-20% in patients with metastatic urothelial cancer (mUC). Most available precision oncology tools rely on tissue-based tumor biomarkers with many challenges in routine clinical practice. A non-invasive liquid biopsy test can be an alternative source. We have developed proprietary Liquid Immuno-Transcriptomics platform (LITOSeek) to identify blood biomarkers that generate patient's immune signatures predictive of clinical outcomes to immunotherapy. This

differentiated solution has been successfully applied to ICI response monitoring in mUC and shows great promise for ICI response prediction. **Methods:** Whole blood samples from 29 patients with BRAF+ and high lactate hydrogenase MM were collected before and after 6-12 weeks of anti-PD-1/CTLA-4 treatment, and 31 patients with mUC were collected before and after 2-6 weeks of anti-PD-1 treatment. Transcriptome profiles were generated by RNA-seq and differentially expressed genes (DEG) were identified by combining differential expression and multivariate analysis on the LITOseek platform. Biological relevancy was assessed by over representation and gene network analysis, and performance was evaluated by Sparse Partial Least Squares (SPLS) regression and cross validation. **Results:** Differential expression analysis (DEA) between responder (R) and non-responder (NR) at baseline identified 119 and 105 DEGs for MM and mBC respectively, that could predict ICI response. Functional analysis of the 119 DEGs of MM indicates upregulation of TCR signaling in R compared to NR, highlighting a more immunogenic tumor. This is further supported by the upregulation of ECM interaction and synthesis genes in NR compared to R, observed both in MM and mUC DEGs lists. SPLS model coupled with PFS analysis indicate highly significant difference at 6-month between the two patient strata for MM (100% R vs 15% NR, $p<0.0001$) and mUC (80% R vs 20% NR, $p<0.01$). Data show that the predictive signature can double the patient responder rate for mUC (40% vs. 20%). **Conclusion:** Capturing immune-related information using next generation sequencing (NGS) and applying cutting-edge machine learning technologies on LITOseekis a promising tool to identify predictive biomarkers of response to ICI in MM and in mUC, as well as to understand the underlying processes. This differentiated solution has demonstrated best-in-class potential to significantly improve patient outcomes in MM and in mUC.

Abstract No: 12

Novel circulating immune biomarkers of response to PD-1/PD-L1 and GSK-3 inhibition

Kelsey Huntington[1], Anna D. Louie[1]; Benedito A. Carneiro[2], Wafik S. El-Deiry[1]

[1]Brown University, Providence, RI, USA
[2]Lifespan Health System, Providence, RI, USA

Introduction: Immune checkpoint blockade (ICB) therapy shows impressive efficacy in microsatellite instability positive (MSI+) colorectal cancer (CRC) but has shown disappointing results in microsatellite stable (MSS) CRC. A growing body of literature characterizes the immunomodulatory roles of glycogen synthase kinase-3 (GSK-3) in the context of anti-tumor immunity. Accordingly, we evaluated the immunomodulatory impact of small-molecule GSK-3 inhibitor 9-ING-41 in combination with ICB in a syngeneic murine model of CRC as well as in peripheral blood samples obtained from patients treated with 9-ING-41 in a phase 1 clinical trial (NCT03678883). Here, we utilized cytokine profiling to identify novel biomarkers of response to therapy. **Methods:** In a syngeneic murine colon carcinoma BALB/c model using MSS cell line CT-26 we compared isotype, 9-ING-41 (70 mg/kg 2x/wk), αPD-1 (10 mg/kg 2x/wk), αPD-L1 (10 mg/kg 2x/wk), 9-ING-41 + αPD-1, and 9-ING-41 + αPD-L1 treatment groups. Using Luminex technology, we investigated the differences in serum cytokine profiles between animals displaying tumor responses (i.e., complete or partial response) and those without response. We also analyzed plasma samples from patients with advanced solid tumors of multiple tissue origins treated with 9-ING-41 that were collected at baseline, 8 and 24 hours post intravenous administration of 9-ING-41. **Results:** Treatment with 9-ING-41 in preclinical studies led to upregulation of tumor cell PD-L1 by western blot analysis, increased anti-tumor immune responses and tumor-infiltrating lymphocytes by flow cytometry and immunohistochemistry, and downregulated angiogenic (VEGF, EGF) and immunosuppressive (TGF-beta) signaling pathways in tumor cells by RNA sequencing. These insights provided the rationale to combine 9-ING-41 with ICB. In this pilot study, we utilized cytokine profiling on murine serum samples and observed that several circulating factors were predictive of response to PD-1/PD-L1 blockade and GSK-3 inhibition. Responders were more likely to have lower serum concentrations of BAFF, CCL7, CCL12, VEGF, VEGFR2, and CCL21 as compared to non-responders. In contrast, responders had higher serum concentrations of CCL4, TWEAK, GM-CSF, CCL22, and IL-12p70 as compared to non-responders. To validate our preclinical results, we utilized human plasma samples from patients treated with 9-ING-41 and correlated cytokine profiles with overall survival (OS) and progression-free survival (PFS). Elevated baseline plasma levels of IL- 1 beta and reduced levels of VEGF correlated with improved PFS and OS among the patients treated with 9-ING-41 and were similarly predictive of response to therapy in the preclinical model. Our data also indicated that PFS was positively correlated with elevated human plasma levels of immunostimulatory analytes such as Granzyme B, IFN-gamma, and IL-2 at 24 hours post-treatment with 9-ING-41. **Conclusion:** We have identified several circulating biomarkers that are predictive of response to GSK-3 inhibition with 9-ING-41 that can be measured prior to or during treatment. These novel biomarkers of response to GSK-3 inhibition could provide significant clinical utility and will be further validated using an expanded cytokine analysis in a larger cohort of patients. In summary, our results 1) provide the rationale for the clinical evaluation of GSK-3 inhibition in combination with ICB and 2) introduce novel biomarkers for correlations with response to therapy.

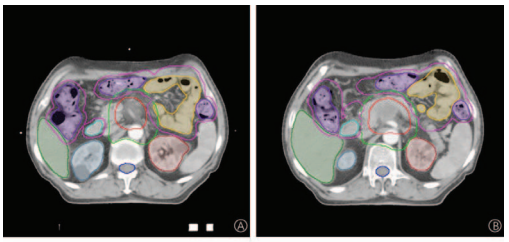

Figure 1 Delineation of target and OAR:Red line: PTV75Gy; Green line: PTV50Gy; Purple line: Planning OAR volumes formed by extravasation of stomach, small intestine, and large intestine

Abstract 14, Figure 1.

Abstract No: 14

Radiotherapy in locally advanced pancreatic cancer with 75Gy simultaneous integrated boost: a dosimetric feasibility study

Ruy Jiang, Zhuang han, Lin Chifang, Wang Jiazhou, Han Xu

Fudan University Shanghai Cancer Center, China

Introduction: This study aims to investigate the feasibility and dosimetric differences between coplanar intensity modulation radiotherapy (CO-IMRT) and non-coplanar intensity modulation radiotherapy (NC-IMRT) when using 75Gy simultaneous integrated boost (SIB) for patients with locally advanced pancreatic cancer (LAPC). **Methods:** Ten patients with LAPC treated with SIB at our

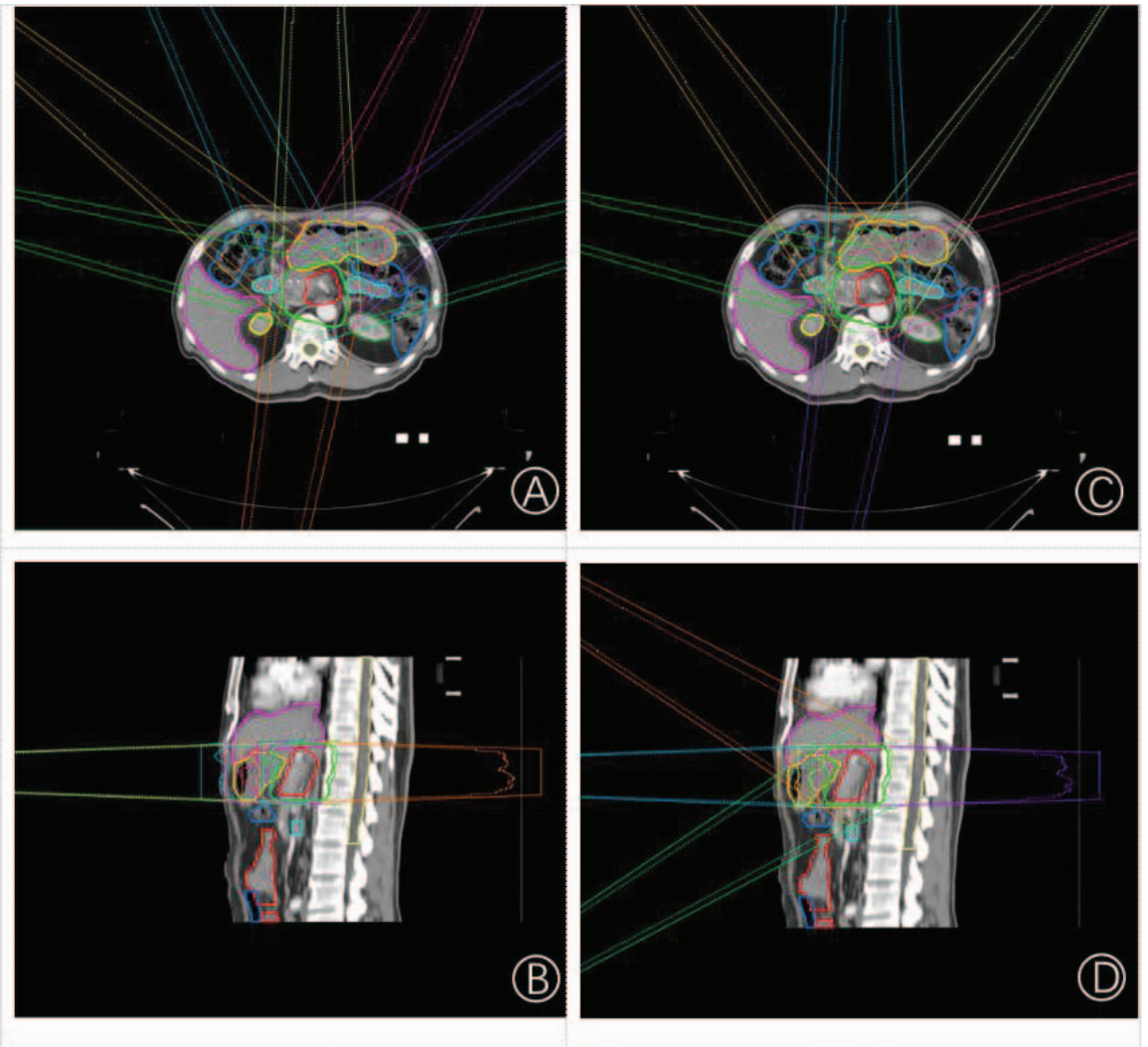

Figure 2 The corresponding transverse and sagittal images of the coplanar field(A and B) and non-coplanar field(C and D) of the same patient.

Abstract 14, Figure 2.

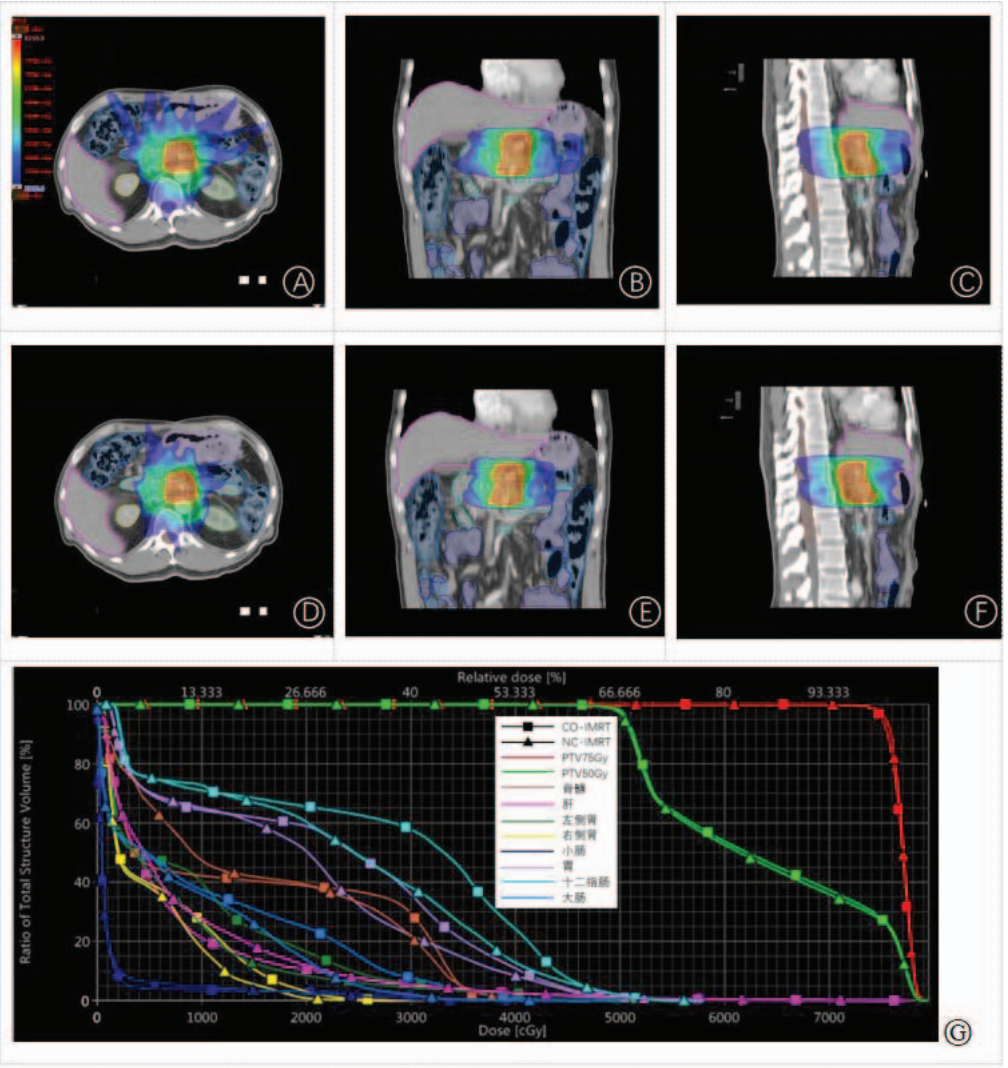

Figure 3 The corresponding dose distribution of transverse, coronal and sagittal images of the coplanar (A, B, C) and non-coplanar(C, D, E) of the same patient and DVH(G)

Abstract 14, Figure 3.

institution were included. The prescribed dose for the PTV_{50Gy} was 50Gy in 25 fractions, and 75Gy in 25 fractions for the SIB PTV_{75Gy}. CO-IMRT and NC-IMRT plans were designed for each patient separately, with identical number of fields, prescription doses and OAR constrains for the same patient. The planning target volume (PTV) dose distribution, conformability index (CI), homogeneity index (HI), indices to OARs for multiple end points, beam-on time and monitor units (MU) were analyzed. Evaluating whether the PTV met clinical requirements and QUANTEC (Quantitative Analysis of Normal Tissue Effects in the Clinic) limits, and comparing dosimetric differences between the two plans. **Results:** Both CO-IMRT and NC-IMRT could achieve the required dose coverage of PTV and meet the QUANTEC dose limits for OARs. The differences between CI, HI, beam-on time and MU of the two plans were not statistically significant ($P>0.05$); NC-IMRT was significantly ($P< 0.05$) decreased bilateral kidney (D_{mean}, V_{12}), liver(V_{30}), small intestine (V_{30},V_{45}), stomach (V_{45}) and large bowel(V_{30}); the other indexes were not statistically significant ($P>0.05$). **Conclusion:** In the treatment of LAPC using 75Gy SIB, both CO-IMRT and NC-IMRT can achieve excellent PTV coverage and meet the OAR constraints in all patients. Without affecting the quality of PTV coverage, NC-IMRT has more advantages in the dose distribution of OARs, which can better protect the OARs and reduce the toxicity to the gastrointestinal tract, liver and kidneys.

Abstract No: 15

Raising the bar for checkpoint inhibitor benefit prediction in non-small-cell lung cancer: Glycoproteomics

Klaus Lindpainter, Apoorva Srinivasan, Alan Mitchell, Apurva Dixit, Gege Xu, Xin Cong, Daniel Serie

InterVenn Biosciences, San Francisco, CA, USA

Introduction: Protein glycosylation is the most abundant and complex form of post- translational protein modification. Glycosylation profoundly affects protein structure, conformation, and function. The elucidation of the potential role of differential protein glycosylation as biomarkers has been limited by the technical complexity of generating and interpreting this information. We have recently established a novel, powerful platform that combines liquid chromatography-mass spectrometry with a proprietary artificial- intelligence-based data processing engine that allows, for the first time, highly scalable interrogation of the glycoproteome. Here we report the performance of this platform to predict likely benefit from immune- checkpoint inhibitor (ICI) therapy in advanced non-small cell lung cancer (NSCLC). **Methods:** Our platform was utilized to assess 532 glycopeptide (GP) and peptide signatures representing 75 serum proteins in pretreatment blood samples from a cohort of 125 individuals (54 females, 71 males, age range 60 to 75 years). Inclusion criteria were as follows: a diagnosis of unresectable stage 3 or 4 NSCLC, treatment with pembrolizumab monotherapy (27 patients), or treatment with combination pembrolizumab-chemotherapy (98 patients). Overall survival (OS) data were available for all patients. Samples and de- identified clinical data were obtained from Tempus Labs (Chicago, IL). **Results:** A multivariable-model-based classifier for OS was created utilizing 70% of the cohort as a training set and seven glycopeptide and non-glycosylated peptide biomarker features selected from a generalized additive model. The classifier yielded a hazard ratio (HR) for prediction of likely ICI benefit of3.96 at $p < 0.0001$. Additionally, the classifier was validated using a test set comprised of the withheld 30% of patients, yielding a HR of 3.86 at $p< 0.01$ which separated patients likely benefiting from ICI therapy from those likely not benefiting from ICI therapy (median OS of 23.2 vs. 5.9 months, respectively, based on classifier score above/below cutoff). **Conclusion:** The glycoproteomic classifier described here predicts with high sensitivity which patients are likely to benefit from ICI therapy. In addition to potentially reducing the use of ICIs in a safe manner in patients who would be unnecessarily subjected to possible adverse drug reactions, our classifier simultaneously has the potential of reducing the burden of health care expenditures. Our results indicate that glycoproteomics holds a strong promise as a predictor for ICI treatment benefit which appears to significantly outperform other currently pursued biomarker approaches.

Abstract No: 16

Identifying cell surface combinations for selectively targeting malignant peripheral nerve sheath tumor cells using a novel single cell combinatorial optimization approach

Matthew Nagy, Rahulsimham Vegesna, Xiyuan Zhang, Sanna Madan, Alejandro Schäffer, Eytan Ruppin, Jack Shern

Cancer Data Science Laboratory, National Cancer Institute, National Institutes of Health, Bethesda, MD, USA

Introduction: Malignant peripheral nerve sheath tumor (MPNST) is an aggressive, treatment resistant, soft tissue sarcoma, with generally poor outcomes. Given recent successes of CAR-T therapy on various solid tumors, there is increased interest in identifying unique surface markers. While no stand-alone surface marker of MPNST has been identified, there is increasing interest in identifying surface gene combinations that may serve as unique biomarkers or targets for this tumor. The objective of this study was to identify cell surface targets that are present on a majority of MPNST cells and minority of non-MPNST cells at a single cell resolution. **Method:** A total of five tissue biopsies from two patients with MPNST collected from the primary tumor (patient 1 only), lung metastasis and normal lung. Single cell RNA sequencing with the 10x Genomics was performed and cells were annotated as MPNST or non-MPNST. A total of 2695 genes previously identified to produce proteins located on the cell surface were evaluated. Mad Hitter, a combinatorial optimization software was utilized to identify cell surface combinations that were present in two scenarios: (Basic scenario) requiring their presence in >80% of MPNST cells and <10% of non-MPNST cells and additionally, (more stringent scenario), to identify combinations that were present on >90% of MPNST cells and <5% of non-MPNST cells. Expression of selected targets were additionally assessed in normal tissues in the genotype tissue expression (GTEX) database to further evaluate their selectivity and potential toxicity. **Results:** Evaluation of the primary tumor from patient one identified DLK1 to be present on >80% of primary MPNST cells and <10% of non-MPNST cells. Increasing the selective stringency requirements, the combinations of SLC39A4, DLK1, and BSG was found to target >95% of MPNST and <1% of non-MPNST cells. Comparing lung metastasis MPNST cells to normal lung tissue cells from the same patient, we find that the best combinations in basic scenario were DLK1 and SLC2A1 (patient one) and MPZ and SLC3A2 (patient two). In the stringent scenario, the optimal combination for patient one was 5 targets (*SLC2A1*, *SLC6A8*, *FGFR1*, *GPC3*, and *DLK1*) and for patient two was 12 targets (*SLC2A1*, *SLC6A8*, *FGFR1*, *GPC3*, *SLC16A1*, *MPZ*, *PCDH7*, *SLC9A3*, *GPM6B*, *SDC2*, *NGFR*, and *TTYH1*). Of the four genes that appeared in both patients, all were >97th percentile in expression compared to all other surface genes. The normal tissues with highest relative expression were nerve

and pituitary tissue, with all four genes being >90th percentile compared to all other surface genes**. Conclusion:** Using a novel computational approach, we identified a combination of three cell surface markers that may target >95% MPNST cells and <1% of non MPNST cells in a single patient. Targeting lung metastasis would require combinations of 2 targets in the basic scenario but 5 and 12 target combinations in the more stringent one, which may be currently impractical. The expression of most of the target surface genes identified is higher in both patients with MPNST than in all normal tissues, but obviously, any future therapeutic approaches exploiting these target combinations should be carefully optimized and evaluated for off target effects. Moreover, while we identify a few common targets, there are clearly individual differences in marker expression, highlighting the need for future personalized therapy.

Abstract No: 17

Early onset cancers in the United Arab Emirates

Pankaj Paul[1], Taleb AlMansoori[1], David Kerr[2], Christopher T. Naugler[3], Garth Powis[1]

[1]Burjeel Medical City, VPS Healthcare, UAE
[2]University of Oxford, Calgary, Canada

Introduction: An increased incidence of cancer in younger individuals <50 years has been observed for a variety of cancers worldwide. This raises important questions when to start screening for cancer, whether there could be different biomarkers or mutations, and whether different cancer therapies might be required for younger compared to older patients. The United Arab Emirates (UAE) has a 45% incidence for all cancers in the age group 20-49 years, which is considerably greater than 8.7% in the USA. There are two different populations of patients with cancer in the UAE; nationals who comprise 28.1% and expatriate 71.9%. Expatriates may return to their home counties as they become older possibly confounding incidence data. **Method:** To better understand the causes of increased cancer risk and early onset breast and colon cancer in the UAE we will perform a three-phase study: In Phase 1 we will conduct a pilot study on 4 UAE national families with known hereditary breast and colon cancer (2 each) and conduct buccal cell germline genetic screening for potential genetic risk factors. In Phase 2 we will use retrospective next generation sequencing of tumor blocks from patients with breast and colon cancer (male and female) ages 25 to 45, and 50-70 years in UAE national and expatriate populations (20 blocks in each group, age and sex matched where possible). In Phase 3 we will prospectively perform white blood cell germline and tumor genomic sequencing using the 500 gene Illumina TrueSight 500 assay, and ATAC-seq for epigenetic changes, in the same age groups of patients with breast and colon cancer. **Results:** Our analysis of UAE DOH data for 2015 show that in the UAE national population 23.8% of colorectal cancer occurs before the age of 50, and 41.9% in the expatriate population, compared to 5.8% for the USA (SEER data 2016), and for breast cancer national population 45.8% and expatriate 60.4%, compared to 12.7% for the USA. **Conclusion:** The trend for the two major cancers in the UAE, colorectal in men and breast in women, is a considerably elevated incidence at age < 50 year compared to USA, with UAE expatriates showing somewhat higher incidences than UAE nationals. A plan is presented how we can better understand the causes of increased cancer risk and early onset breast and colon cancer in the UAE national and expatriate populations.

Abstract No: 18

KRAS G12C–STK11 co-mutated lung adenocarcinomas: Are there new hopes for targeted immunotherapy?

Radu Pirlog[1, 2], Nicolas Piton[2], Florent Marguet[2], Aude Lamy[2], Jean-Christophe Sabourin[2], Ioana Berindan-Neagoe[1]

[1]Research Center for Functional Genomics, Biomedicine and Translational Medicine, Iuliu Hatieganu University of Medicine and Pharmacy, Cluj Napoca, Romania
[2]Pathology Department and INSERM U1245, Rouen University Hospital, Normandy University, Rouen, France

Introduction: A new molecular target in lung adenocarcinomas (LUADs) is represented by the glycine-to-cysteine mutation at position 12, codon 34 (KRAS G12C) that is present in approximatively 13% of cases. In 2021 two molecules were approved that target KRAS G12C mutated LUAD, Sotorasib and Adagrasib, showing a partial response rate of 33,9% for Sotorasib and an overall response of 45% for Adagrasib. Results are promising, but there is still a large group of KRAS G12C LUAD that don't benefit from these molecules. Therefore, there is a need for a better characterization of the molecular landscape of these tumors in order to improve the patient selection. A possible subgroup of responders is represented by the co-mutated KRAS G12C–STK11 LUADs that showed promising results in clinical trials. **Method**: We aim to characterize a new molecular subtype of KRAS G12C LUADs that are also harboring a mutation in the STK11 gene using classic histology, immunohistochemistry and next generation sequencing NGS). Samples from 51 patients diagnosed through NGS with a co-mutation KRAS G12C and STK11 were included in our study. Each case was individually assessed by two pathologists for morphological parameters: histology, tumor cellularity, nuclear atypia, presence of necrosis and tumor infiltrating lymphocytes (TIL). Routine diagnostic immunohistochemistry was performed on a BENCHMARK ULTRA Ventana-Roche. NGS was performed on a MiSeq sequencer (Illumina©) and the gene library was prepared with the kit Tumor

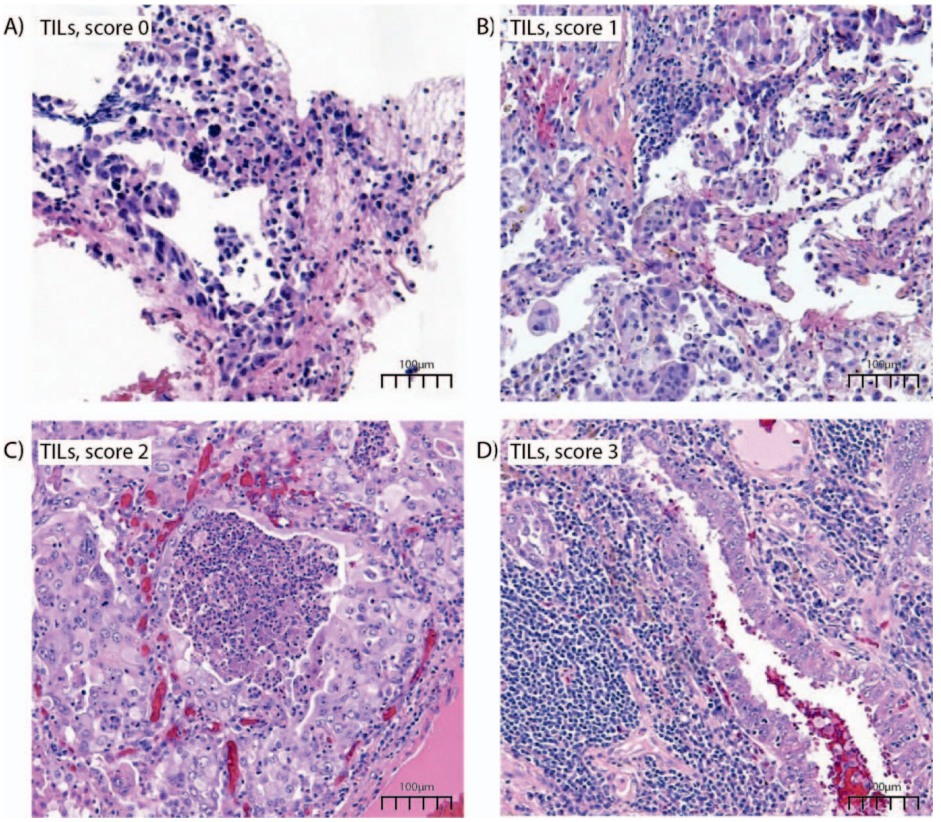

Abstract 18, Figure 1.

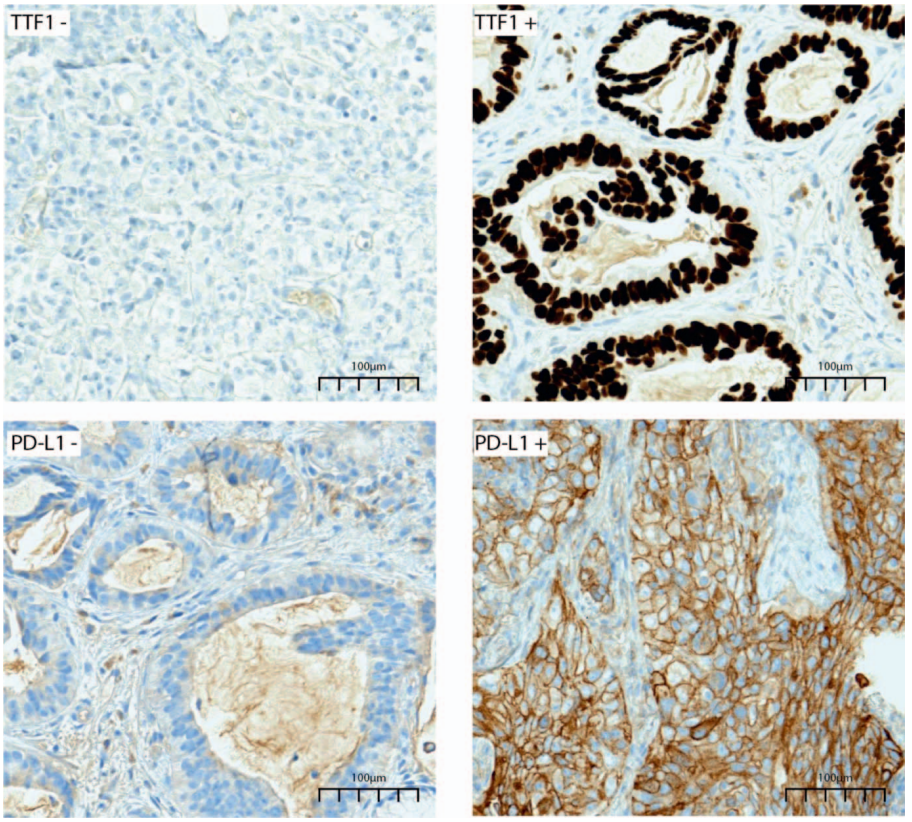

Abstract 18, Figure 2.

Hotspot MASTR Plus (Multiplicom®). **Results:** The mean age was 62.2-year-old. The sex distribution included 33.33% males and 64% females. The main histology findings were acinar in 39.21% and no other specified (NOS) in 21.5% of samples. TILs were evaluated as high in 39.51% of cases and moderate in 27.45% of cases. Necrosis was present in 23.52% and nuclear atypia in 31.37% of samples. TTF1 immunohistochemistry was positive in 64.51% of samples and PD-L1 was positive in 19.6% of samples. NGS analysis identified additional mutations in multiple genes including *ALK*, *CDK2NA*, *CTNNB1*, *DDR2*, *FGFR3*, *MET*, and *PIK3CA*. **Conclusion**: We realized a complex characterization of a specific subgroup of KRAS G12C-STK11 co-mutated LAUDs that could have an improved response to KRAS G12C inhibitors. This result is of high interest as previously STK11 mutated LUADs were associated with a poor prognosis, reduced PD-L1 positivity and resistance to anti-PD1 / antiPD-L1 blockade.

Abstract No: 19

Is NGS the new golden standard for ALK Testing? The diagnostic journey of an atypical case

Radu Pirlog[1,2], Nicolas Piton[2], Florent Marguet[2], Aude Lamy[2], Jean-Christophe Sabourin[2], Ioana Berindan-Neagoe[1]

[1]Research Center for Functional Genomics, Biomedicine and Translational Medicine, Iuliu Hatieganu University of Medicine and Pharmacy, Cluj-Napoca, Romania
[2]Pathology Department and INSERM U1245, Rouen University Hospital, Normandy University, Rouen, France

Introduction: ALK gene rearrangements is a major alteration in lung adenocarcinoma (LUAD) present in about 5% of cases. Identification of ALK rearrangements is routinely done by immunohistochemistry (IHC) followed by fluorescent in situ hybridization (FISH) using break-apart probes, considered as the golden standard. However, multiple discordances between IHC and FISH analyses have been reported leading to questioning the sensitivity and specificity of the FISH. **Methods:** We present a case of a patient diagnosed in 2013 with a pulmonary tumor situated in the lower lobe of the right lung. In 2018 the patient was diagnosed with a metastasis at the level of left lung. The surgical specimens were processed according to standard protocols. Routine hematoxylin-eosin staining and lung diagnostic IHC was made. IHC for ALK was perform using clone D5F3 (Roche-Ventana).

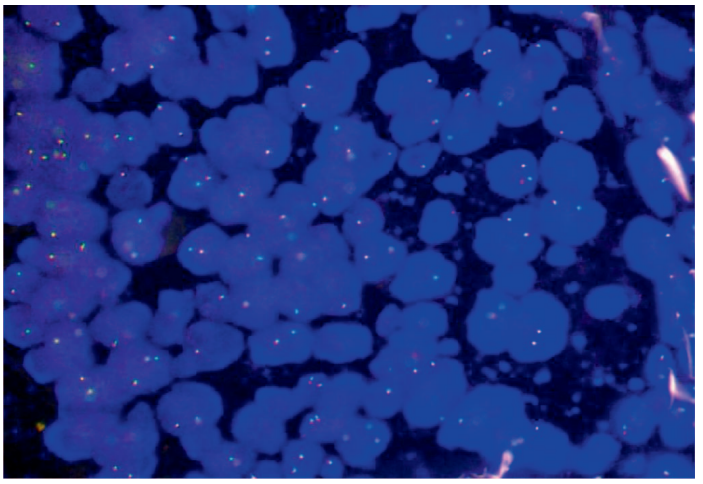

Abstract 19, Figure 1. FISH analysis, 100x of the LUAD. We notice the loss of red spot in the majority of the cancer nuclei.

FISH analysis was carried out using Vysis ALK Break Apart FFPE FISH Probe Kit © and EGFR, KRAS and BRAF mutations were researched by SNaPshot®. In 2021 the molecular analysis was carried out using Archer® FusionPlex Lung panel kit, on a MiSeq sequencer (Illumina), and the data were analyzed with the Archer® Analysis software. **Results:** In 2013 the right inferior lobe resection showed an infiltrative LUAD, acinar type with a micro-papillary contingent, pT2aN0MxL0N0V0. The tumor was ALK positive on IHC and negative on FISH. Molecular biology analysis was negative for EGFR, KRAS and BRAF. In 2018 on the left basal pulmonary resection was identified a 9 mm LUAD acinar type with a component of micro-papillary contingent, histologically compatible with the primary lesion from 2013 pT2aN0MxL0N0V0. The tumor was intensively positive for ALK on IHC and negative on FISH. Interestingly, the FISH analysis revealed a loss of the red spot in 75% of the nuclei analyzed (Figure 1). Molecular biology analysis was still negative. In NGS analysis using the Archer® FusionPlex Lung panel kit (Archer®) revealed a fusion between ALK exon 2 - EML3 exon 13 (Figure 2). The case was presented in the regional tumor bord and a targeted therapy for ALK inhibitors was considered. **Conclusion:** This case emphasized an atypical EML4-ALK fusion which was not detected by break-apart conventional FISH. We highlight the need for a new gold standard for ALK rearrangements testing represented by ARN NGS, a more sensitive approach that could identify patients with rare molecular phenotypes.

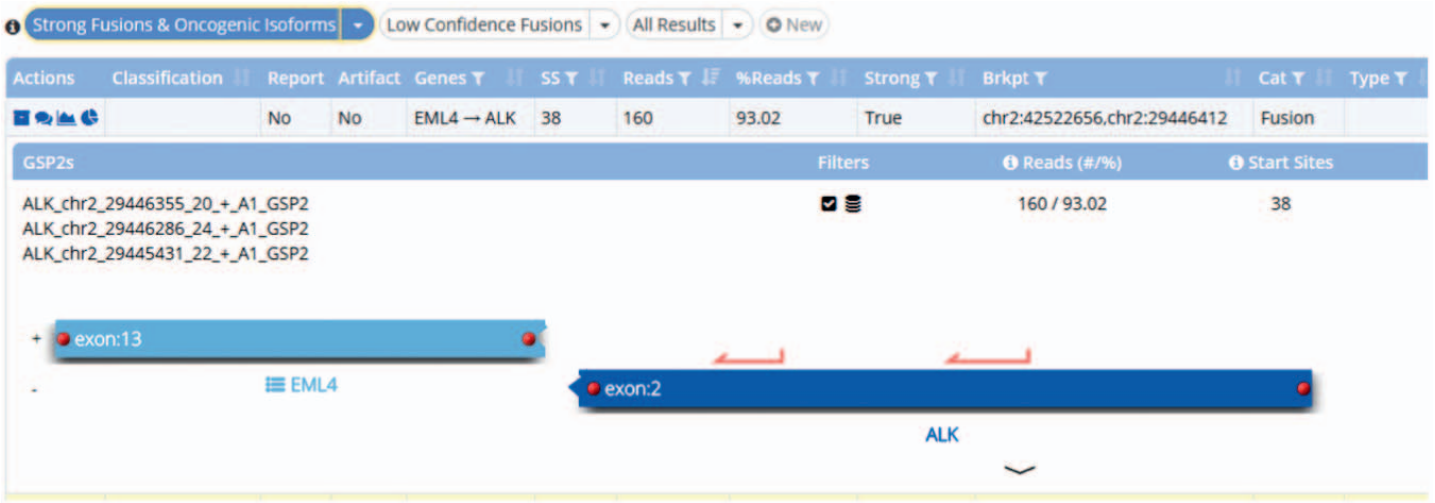

Abstract 19, Figure 2. NGS analysis using RNA Archer FusionPlex Lung Kit. A gene fusion was detected between exon 2 of the ALK gene and exon 13 of the EML4 gene. This translocation is not detectable by classic FISH analysis as the break-apart detection kit that is focusing on exon 20.

Abstract No: 20

Circulating tumor DNA as a biomarker of surgical treatment effectiveness in patients with colorectal or breast cancer

Anastasiia Pryvalova, Vitaliia Kostiuchenko, Ihor Vynnychenko

Sumy State University, Ukraine

Introduction: Circulating tumor DNA (ctDNA) are fragments of nucleic acid released into the bloodstream by dying cancer cells. It contains unique somatic mutations, and recent studies demonstrate that they can give essential information about available solid tumors. ctDNA detected in the peripheral blood sample allows prediction and monitoring of the disease dynamics by monitoring treatment flow and detecting minimal residual disease. We are confident that increasing the amount of information in this area will play a significant role in further cancer diagnostic development. Our study aimed to evaluate the prognostic role of ctDNA for monitoring the effectiveness of surgical treatment for patients with colorectal cancer (CRC) or breast cancer (BC). **Method**: Samples of tumor tissue, fixed in formalin and embedded in paraffin (screening samples), and ctDNA from plasma of 30 patients with CRC and 38 patients with BC were used for the study. Only patients who were planned for radical surgery were selected. Somatic mutations in the *BRAF*, *KRAS*, *PIK3CA*, and *TP53* genes were used as markers of the disease for CRC, and *PIK3CA* and *TP53* genes were used for BC. Plasma samples taken before and after radical surgery were examined. Quantitative determination of gene mutations was performed by digital PCR using QuantStudio 3D Digital PCR (Applied Biosystems, USA) and appropriate Thermo Fisher software. **Results**: Investigating mutations were found in 73.3% of samples of patients with CRC. 63.6% (14/22) of these patients had only one mutation (KRAS - 27.3%, TP53 -22.7%, BRAF - 4.5%, PIK3CA - 9.1%) and 36.4% (8 / 22) had different combinations of desired mutations. The most commonly genes combined with the *TP53* gene. Mutations in the *PIK3CA* and *TP53* genes in combination or alone were detected in 44.7% of patients (17/38) with BC. In one case, a mutation in both genes was detected at once, and all other patients had only one of the two studied mutations. The mutation rate of the *PIK3CA* gene was 28.95%, and the *TP53* gene was 18.4%. The results of the determination of the somatic mutations in the *PIK3CA* and *TP53* genes in the plasma ctDNA of patients with BC and the *BRAF*, *KRAS*, *PIK3CA*, and *TP53* genes in the plasma ctDNA of patients with CRC were comparable with the results obtained from histological samples. This fact indicates that mutations detected in tumor tissue were determined in the plasma ctDNA of the respective patient. The dynamic of changes of ctDNA levels demonstrated a significant decrease or disappearance of ctDNA in samples taken after surgery. This was observed for all desired mutations**. Conclusion:** Quantitative changes in mutated ctDNA of blood plasma can reflect the effectiveness of surgical treatment in patients with CRC and BC. It is planned to assess the dynamics of ctDNA in the long term to identify possible recurrence of the disease.

Abstract No: 21

Subtype-specific and biomarker-driven treatment for peripheral T-cell lymphomas: A phase II multi-cohort study

Manju Sengar[1], Hasmukh Jain[1], Epari Sridhar[1], Tanuja Shet[1], Akhil R[2], Archi Agrawal[1], Lingaraj Nayak[1], Sangeeta

Kakoti[1], Siddhartha Laskar[1], Lingaraj Nayak[1], Bhausaheb Bagal[1]

[1]Tata Memorial Hospital, Mumbai, India
[2]Adyar Cancer Institute, India

Introduction: Most common subtypes of mature T-Cell lymphomas include: Angioimmunoblastic T-cell lymphomas (AITL), PTCL with T-follicular helper (TFH) phenotype and ALK-negative anaplastic large cell lymphoma (ALCL). Outcomes of majority of PTCLs except ALK positive ALCL remain poor with 5-year overall survival of 32% with CHOP/CHOP-like chemotherapy. Treatment for PTCLs have been extrapolated from the trials of other aggressive NHLs, making CHOP the de-facto standard of care. Attempts to improve outcomes include addition of etoposide or brentuximab vedotin (BV). However, the benefit is limited to ALCL and PTCL subtype. The main challenge is achievement of complete response and short-lived complete responses. **Objectives:** Therefore, there is a need for effective treatment options during induction and maintenance to improve the outcomes. Despite the improved understanding of the underlying molecular pathways, the treatment strategies have been subtype- agonistic. Hence it is pertinent to explore subtype-specific biomarker-based. **Methods:** It will be a single center, phase II study evaluating the efficacy and safety of biomarker driven therapy in cohorts of T-follicular helper cell lymphomas and PTCL- NOS subtypes. The primary objective of this study is to evaluate the complete response (CR) rates in the cohorts of T-follicular helper cell lymphomas and PTCL-NOS subtypes. Secondary objectives include assessment of safety, progression-free and overall survival. The exploratory objectives would include correlation of outcomes with total metabolic tumor, circulating tumor DNA at different time points and molecular profile. This trial will include patients with histologically confirmed diagnosis of nodal T cell lymphoma with Follicular helper (TFH) phenotype (tumor cells must express 2 or 3 TFH-related antigens, including PD1, CD10, BCL6, CXCL13, ICOS and CCR5) and PTCL- NOS. Lymphomas with TFH phenotype includes Angioimmunoblastic T Cell lymphoma, Follicular T cell lymphoma and T follicular helper (TFH) variant (5). Patients in the 18-70 age group with ECOG PS $\leq$ 3 with optimal organ functions will be included. Patients with active viral infections (HIV, HCV and HBV), CNS involvement by lymphoma would be excluded. The treatment will be based on the subtype and all patients will be subcategorized into four cohorts. Cohort 1: It will include patients with TFH lymphomas. These patients will be treated with Tab Azacitidine 300 mg once a day for 14 days and Cap Cyclosporin 50 mg BD daily both as induction therapy for 6 months and 1 year as maintenance therapy in patients who continue to respond without significant toxicity. Cohort 2: It will include PTCL-NOS patients with TBX21 overexpression. These patients will be treated with Bortezomib, Etoposide, Adriamycin, Cyclophosphamide and Prednisolone(V-EPCH), every 21 days for 6 cycles. This will be followed by maintenance with 6-mercaptopurine at 50 mg once daily (titrated based on ANC and platelet) for a total of 1 year. Cohort 3: This cohort will include PTCL-NOS patients with GATA3 expression. These patients will be treated with Bortezomib, Pomalidomide and Dexamethasone for 6 cycles followed by Bortezomib and Pomalidomide maintenance for 1 year. Cohort 4: This cohort will include PTCL NOS patients who do not have TBX21 expression or GATA3 expression and have cytotoxic profile. These patients will be treated with pegylated asaparaginase, Gemcitabine, and Oxaliplatin administered once every 21 days for 6 cycles. This will be followed by maintenance with 6MP 50 mg daily (titrated based on ANC and platelet) for a total of 1 year. Response assessment: All cohorts will undergo response assessment after cycle 4 with PET-CT. Those who remain in partial response will be evaluated for response after cycle 6. Subsequently the PET-CT will be done once in 4 months for next two years or earlier in cases of clinical suspicion of disease progression (in all cohorts). Response and progression will be evaluated in this study using the Lugano criteria for lymphoma response assessment. This study would be based on Simon's two stage (minimax) design with boundaries for efficacy and futility based on historical data with CHOP chemotherapy in these regimens. A total of 130 patients would be included in this study across all cohorts. Conclusion: With the above approach we aim to identify the active regimen for each of the cohort based on the complete response rates. If the CR rates cross the predefined boundary then that particular treatment regimen will be tested in a phase III trial.

Abstract No: 22

RNA sequencing and comprehensive analytics to enhance personalized cancer treatment decision-making

Anton Buzdin[1], Alexey Moisseev[1], Elena Poddubskaya[1], Maxim Sorokin[2], Andrew Garazha[3], Maria Suntsova[1], Maxim Kovalenko[4], Alexander Seryakov[5], Marina Sekacheva[1]

[1]Sechenov University, Moscow, Russia
[2]Oncobox Ltd., Moscow, Russia
[3]OmicsWay Corp., Walnut, CA, United States
[4]Moscow Institute of Physics and Technology, Dolgoprudny, Russia
[5]Medical Holding SM-Clinic, Moscow, Russia

Introduction: Standard genetic profiles of tumor biosamples are not clinically actionable in 80-90% of patients with cancer. RNA sequencing (RNAseq) is an alternative robust tool for evaluating tumor molecular portraits that can potentially complement available genetic tests**. Method:** We developed a cloud-based bioinformatic

platform Oncobox that analyses whole exome and transcriptome sequencing data of FFPE tumor biopsy samples to generate a personalized report supporting a treatment decision. Oncobox builds a rating of targeted cancer drugs prioritized according to their predicted efficacy. We validated this approach in a series of retrospective trials and investigated clinical relevance of the RNA-based predictions in a prospective trial including patients with advanced solid tumors. **Result:** We showed that FFPE RNAseq data enable robust assessment of expression levels of widely used cancer IHC biomarkers (PD-L1, HER2, ER, PGR). FFPE RNAseq also can be used for detection of known and novel cancer fusion transcripts. FFPE RNAseq data can be used to robustly estimate tumor mutation burden. In retrospective trials, Oncobox efficacy was demonstrated for predicting individual tumor response in glioblastoma, gastric and colorectal cancers. We then initiated prospective clinical trial NCT03724097 with 239 advanced solid tumors not responding on the standard therapy, for which FFPE RNAseq data were obtained and analysed using Oncobox platform. Treating doctors either followed the platform recommendations (Oncobox group, n=38) or not (control group, n=28). Control over disease (RECIST CR+PR+SD) was observed in 76% of the patients from the Oncobox group vs 50% in the control group (Fisher P = 0.037), when the analysis was restricted to recent biopsies. We also observed differential progression-free survival (PFS) trends between these two groups with HR = 0.38 (P = 0.008). **Conclusion:** Comprehensive analytic and experimental RNAseq-based panel Oncobox has potential to improve control-over-disease and PFS characteristics for targeted therapeutic treatment of advanced solid tumors. Using recent biopsies is essential to obtain robust estimates of targeted drug efficiencies.

Abstract No: 23:

MYC inhibition by OMO-103 induces immune cell recruitment in preclinical models of NSCLC and modulates the cytokine and chemokine profiles of Phase I patients

Laura Soucek[1], Sílvia Casacuberta-Serra[2], Sandra Martínez-Martín[2], Íñigo González-Larreategui[1], Sergio López-Estévez[2], Toni Jauset[2], Mariano F. Zacarías-Fluck[1], Daniel Massó-Vallés[2], Génesis Martín[1], Laia Foradada[2], Judit Grueso[1], Erika Serrano del Pozo[1], Hugo Thabussot[2], Virginia Castillo Cano[2], Jonathan R. Whitfield[1], Manuela Niewel[2], Marie-Eve Beaulieu[2]

[1]Vall d'Hebron Institute of Oncology (VHIO), Barcelona Spain
[2]Peptomyc L.A., Spain

Introduction: Despite the promise of targeted therapies and immunotherapy, many patients with cancer do not respond to treatment and are still in need of effective therapeutic options. We propose a revolutionary strategy based on the inhibition of MYC, a central molecule that drives multiple aspects of tumor progression and immune evasion. Although MYC has long been considered undruggable, we have demonstrated the safety and dramatic therapeutic potential of its inhibition using a MYC dominant negative, termed Omomyc. We showed that the Omomyc mini-protein abrogates tumor progression in a KRAS-driven Non-Small Cell Lung Cancer (NSCLC) mouse model, modulates chemokine/cytokine profiles and recruits T cells to the tumor site. These results have granted further development of the Omomyc mini-protein towards ongoing Phase I/IIa clinical trials. **Methods:** We used a well-characterized $Kras^{G12D}$ transgenic NSCLC mouse model, a syngeneic $Kras^{G12V}/p53^{KO}$ NSCLC mouse model and PBMC-humanized KRAS and EGFR-driven xenograft mouse models. Tumor growth was measured by microCT or caliper measurements. Immune cell infiltration was evaluated by immunohistochemistry and flow cytometry. In addition, patient samples were obtained from the ongoing Phase I study and soluble immune modulators were measured by Luminex®. **Results:** Here we show for the first time that, in our preclinical models, the infiltrating T cells consequence of Omomyc treatment are mainly $CD4^+$ T cells expressing PD-1, Tim-3, OX-40 and 4-1BB, suggesting that Omomyc induces the expansion of this tumor-reactive cell population. Interestingly, mice treated intranasally with Omomyc display higher proportions of Th1- Th17 hybrid population, effector memory T cells, cytolytic NK cells and activated dendritic cells. Importantly, this immune stimulatory effect is also observed upon systemic intravenous Omomyc administration in a p53/KRAS-mutated NSCLC model. Finally, we confirmed that Omomyc treatment also induces $CD4^+$ and/or $CD8^+$ T cell recruitment in PBMC- humanized xenograft lung cancer models independently of their driving mutation. Most notably, immune engagement was also seen in Phase I patients receiving OMO-103 and showing stable disease after 9 weeks of treatment. In particular, they display a cytokine signature that was not observed in patients with progressive disease. In addition, OMO-103 treatment also modified serum levels of other soluble immune modulators, including *bona fide* MYC targets. Of note, none of the patients showed anti-drug antibodies throughout the treatment. **Conclusion:** Our findings support the therapeutic opportunity to induce a potent antitumor immune response in NSCLC by pharmacological MYC inhibition with Omomyc. In addition, they suggest that OMO-103 can also induce immune activation in patients displaying stable disease.

Abstract No: 24

A framework for incorporating prior knowledge in feature selection for precision oncology

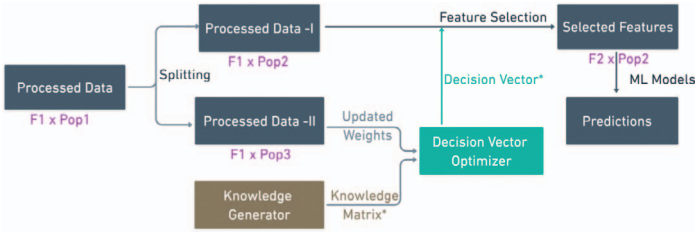

Abstract 24, Figure 1. A hybrid framework for feature selection by composing data-driven and problem-specific knowledge-driven approaches. The green rectangle for method (II) and the brown for method (I). Pink variables represent the dimensions. The rectangles for products and the text between the process.

Kartheeswaran Thangathurai, Stanislav Engel, Nadav Rappaort, Eitan Rubin

Ben-Gurion University of the Negev, Be'er Sheva, Israel

Introduction: For many algorithms that try to build drug response predictors, feature selection was shown to improve the predictivity and generality of the resulting classification models. Several mechanisms have been proposed for data-driven feature selection. Alternatively, prior knowledge-driven feature selection has also been proposed. However, the problem of combining data-driven and prior-knowledge-driven feature selection has not been extensively discussed. **Method:** A framework is proposed that combines prior knowledge-based feature selection with data-driven feature selection: (I) collect related knowledge from various available sources online and offline to generate a Knowledge Matrix. The knowledge matrix holds multiple vectors, each representing one type of prior knowledge about each feature. The knowledge matrix holds k x n values, where k is the number of knowledge vectors, each containing information about n features. (II) Decision Vector Optimization. In this step, a weights vector is learned from the data to extract from the knowledge matrix a decision vector (a binary vector of length n) which defines if a feature is to be used or not. We propose that prior knowledge utilization can be achieved by data-driven, task-specific optimizing of the weights vector, which defines how the knowledge matrix is translated into a decision vector. This step is task-specific, such that two different classification tasks will generate different feature weights. **Result**: A framework that combined data and prior knowledge together to make feature selection as shown in Figure 1. **Conclusion**: We define a hybrid process that combines prior knowledge and data for feature selection. We discuss possible mechanisms to address some of the relevant challenges to its implementation. Such a framework can be useful in knowledge-rich fields such as prediction oncology, or for any task where the size of the feature space and the knowledge space is a problem. We specifically discuss how this approach can help predict drug response in oncology.

Abstract No: 25

Implementation of the Avera/Sema4 oncology and analytics protocol (ASAP)

Casey B. Williams[1], David Starks[1], Rachel Elsey[1], Tobias Meissner[1], Benjamin M. Solomon[1], Tomi Jun[2], Melanie Albano[2], Feras Hantash[2], Eric Schadt[2], Luis Rojas-Espaillat[1], John H. Lee[1], William K. Oh[2,3]

[1]Avera Cancer Institute, Sioux Falls, SD, USA
[2]Sema4, Stamford, CT, USA
[3]Tisch Cancer Institute, Division of Hematology/Medical Oncology, Icahn School of Medicine at Mount Sinai, New York, NY, USA

Introduction: Precision medicine represents a new era in oncology and population health. Comprehensive molecular profiling and hereditary cancer testing are increasingly important in the routine management of many malignancies, yet may not be widely adopted in many practices and leads to patients not consistently receiving care recommended by current national guidelines such as NCCN and ASCO. In addition, available targeted DNA sequencing panels may be limited to only defined drivers and lack detection in precancerous conditions. Whole exome sequencing (WES) combined with whole transcriptome sequencing (WTS) represent an expanded testing approach that identifies additional genetic changes beyond standard commercial panel tests. Current evidence suggests that WES/WTS is feasible to carry out in routine clinical practice, with improved detection of somatic alterations compared to smaller panels, and the promise to enhance access to targeted therapies and clinical trials. The primary purpose of the ASAP study is to understand the breadth of molecular characteristics present in participants cared for in a large integrated community-based health system, by linking comprehensive molecular profiles with clinical data extracted and curated from the electronic medical record. **Methods:** Enrolled participants are expected to receive WES/WTS and proteomics on their primary tumor and metastatic sites where feasible as well as hereditary testing, pharmacogenomics (PGx) and microbiome profiling. Liquid biopsies will be performed every 3 months while on treatment or when treatment is changed, in follow up to coincide with scheduled radiographic testing, and as part of annual routine surveillance. For participants not diagnosed with cancer, each participant will receive hereditary testing, PGx, microbiome, and a liquid biopsy at least annually. Participants also consent to sharing their electronic health information. Future stages of this work will employ natural language processing (NLP) methods to develop algorithms to help identify opportunities to improve patient outcomes. Projected enrollment is 1000 participants in year 1, 1500 participants in year 2, and up to 3000 annually thereafter. Clinical trial information: NCT05142033. **Results:** The ASAP study

Abstract 25, Figure 1.

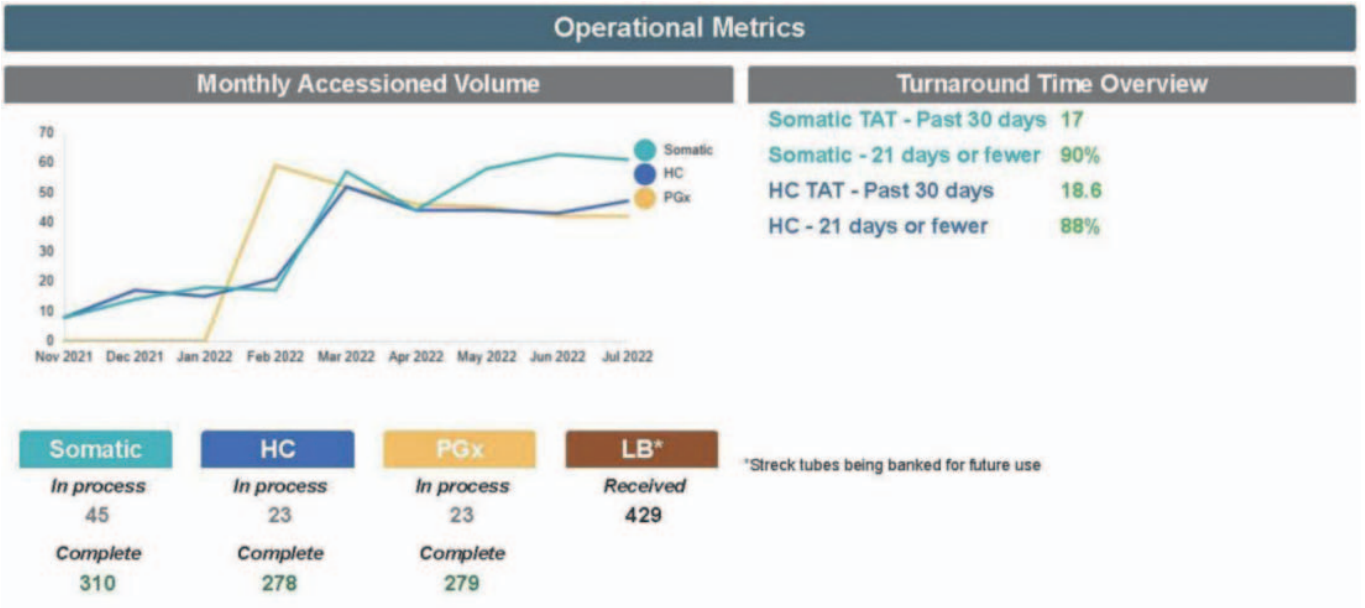

Abstract 25, Figure 2.

was initiated in November 2021 and is open and actively enrolling. The study is anticipated to be open to accrual for 5 years. As of August 2022, the study has enrolled over 300 pts and is expanding outside of Sioux Falls to additional cancer centers in the Avera footprint. Every patient enrolled is formally evaluated via our molecular tumor board and numerous research analysis are underway. Updated results will be provided at the meeting. **Conclusion:** The ASAP study has multiple aims, but the primary objective is to understand the breadth of molecular characteristics present in participants cared for in a large integrated community-based health system, by linking comprehensive molecular profiles with clinical data extracted and curated from the electronic medical record with the goal to improve clinical outcomes and provide a fertile repository for quality improvement and real-world data investigations. We plan to achieve this by:

- o Democratizing access to molecular testing for patients with cancer regardless of stage disease or pre-malignant conditions
- o Combining hereditary, whole exome, and transcriptome comprehensive molecular profiling with advanced healthcare informatics to deliver standard of care precision oncology while exploring feasibility and value of novel multi-omic data and models
- o Expanding our longitudinal Real-World Outcomes database to better inform and evaluate the safety, efficacy, and tolerability of cancer therapeutics
- o Further developing algorithms and tools to inform the clinician on treatment selection or intervention and matching clinical trials

Abstract No: 26

Integrative genomic and transcriptomic analysis reveals immune subtypes and prognostic markers in ovarian clear cell carcinoma

Shuang Ye[1,2], Qin Li[2,3], Yutuan Wu[1,2], Wei Jiang[1,2], Shuling Zhou[2,4], Xiaoyan Zhou[2,4], Wentao Yang[2,4], Xiaoyu Tu[2,4], Boer Shan[1,2], Shenglin Huang[2, 3], Huijuan Yang[1,2]

[1]Department of Gynecologic Oncology, Fudan University Shanghai Cancer Center, Shanghai, China
[2]Department of Oncology, Shanghai Medical College, Fudan University, Shanghai, China
[3]Fudan University Shanghai Cancer Center, and the Shanghai Key Laboratory of Medical Epigenetics, Institutes of Biomedical Sciences, Fudan University, Shanghai, China
[4]Department of Pathology, Fudan University Shanghai Cancer Center, Shanghai, China

Introduction: Ovarian clear cell carcinoma (OCCC), as a histologic subtype of epithelial ovarian cancer, has distinctive clinical and biological behaviour. OCCC represents a great challenge and unmet need given its disease aggressiveness and chemotherapy resistance. We performed an integrative genomic and transcriptomic profiling to identify molecular subtypes and prognostic markers with special focus on immune-related pathways. **Method:** Totally, 50 Chinese patients were subjected to targeted next-generation sequencing and transcriptomic sequencing. **Results:** Two distinct subgroups were identified as immune (22.0%) and non-immune (78.0%) based on the immune-pathway related hierarchical clustering. Surprisingly, patients with immune subtype had a significantly worse survival. The prognostic capacity was validated in external cohorts. The immune group had higher expression of genes involved in pro-inflammation and checkpoints. PD-1 signalling pathway was enriched in the immune subtype. Besides, the immune cluster presented enriched expression of genes involved in epithelialmesenchymal transition, angiogenesis and PI3K-AKT-mTOR signalling, while the non-immune subtype had higher expression of metabolic pathways. The immune subtype had a higher mutation rate of PIK3CA though significance was not achieved. Lastly, we established a prognostic immune signature for overall survival. Interestingly, the immune signature could also be applied to renal clear cell carcinoma, but not to other histologic subtype of ovarian cancer. **Conclusion:** An immune subtype of OCCC was identified with poor survival and enrichment of PD-1 and PI3K-AKT-mTOR signalling. We constructed and validated a robust prognostic immune signature of patients with OCCC.

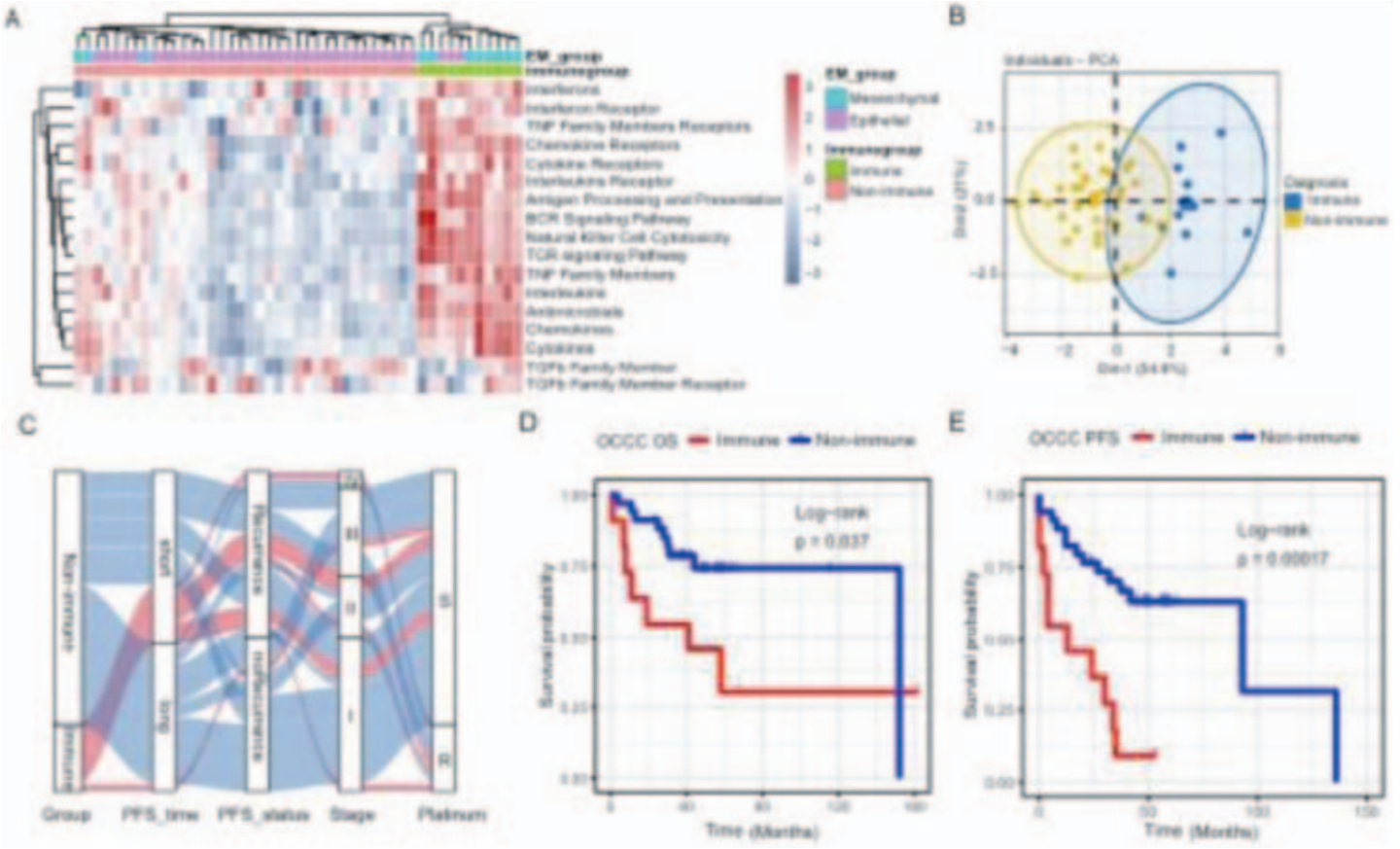

Abstract 26, Figure 1. Immune-pathway-based subtyping of ovarian clear cell carcinoma (OCCC) and clinical implications.

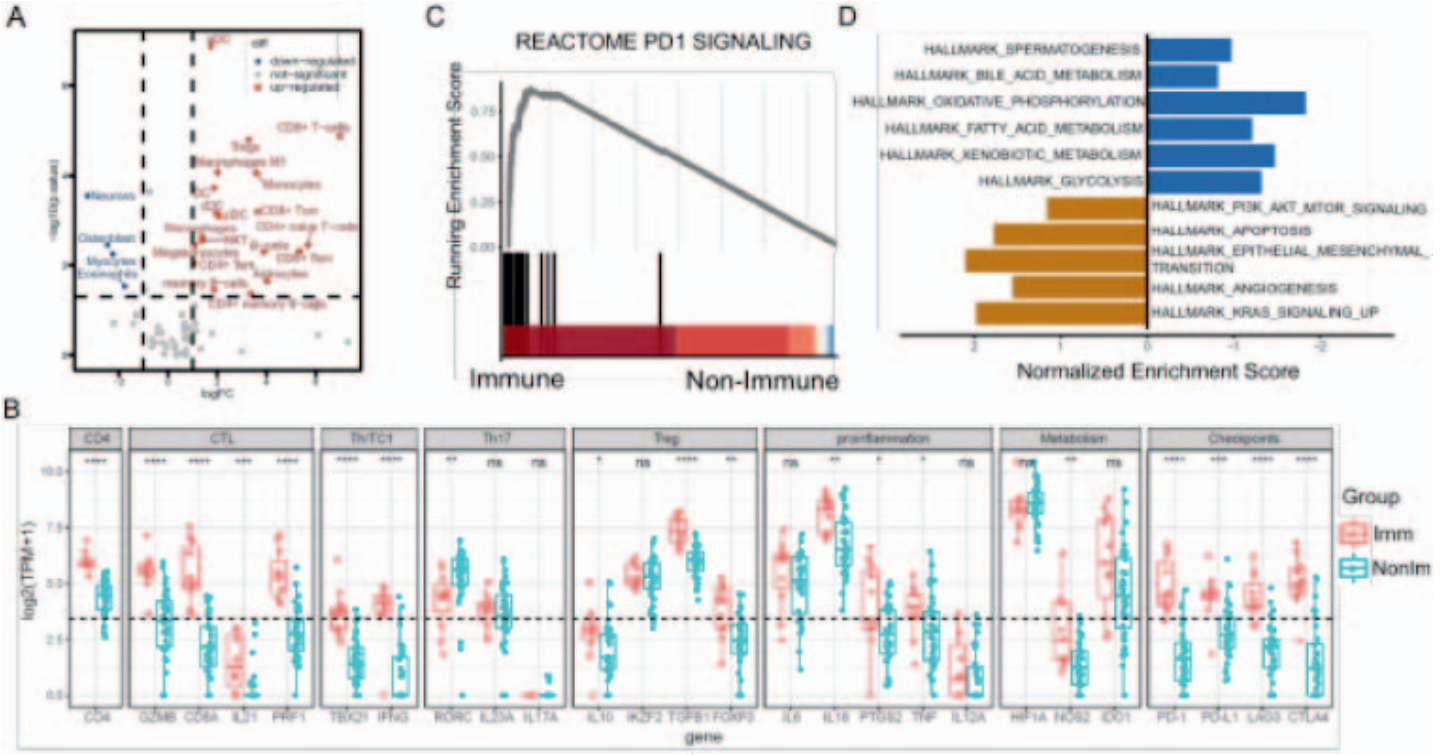

Abstract 26, Figure 2. Comparison of features between the immune and non-immune group.

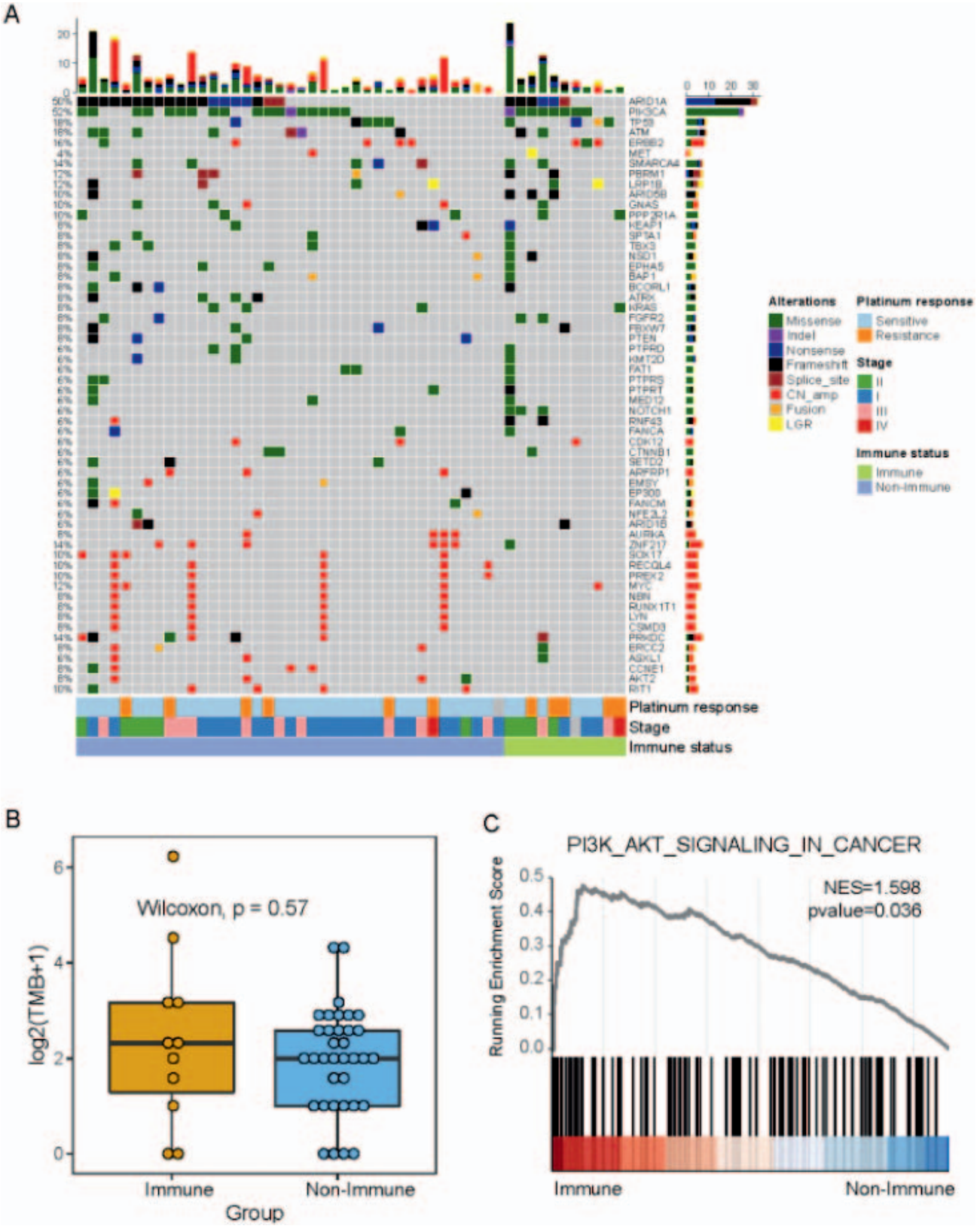

Abstract 26, Figure 3. The significance of genomic mutations in the two immune subtypes of OCCC.

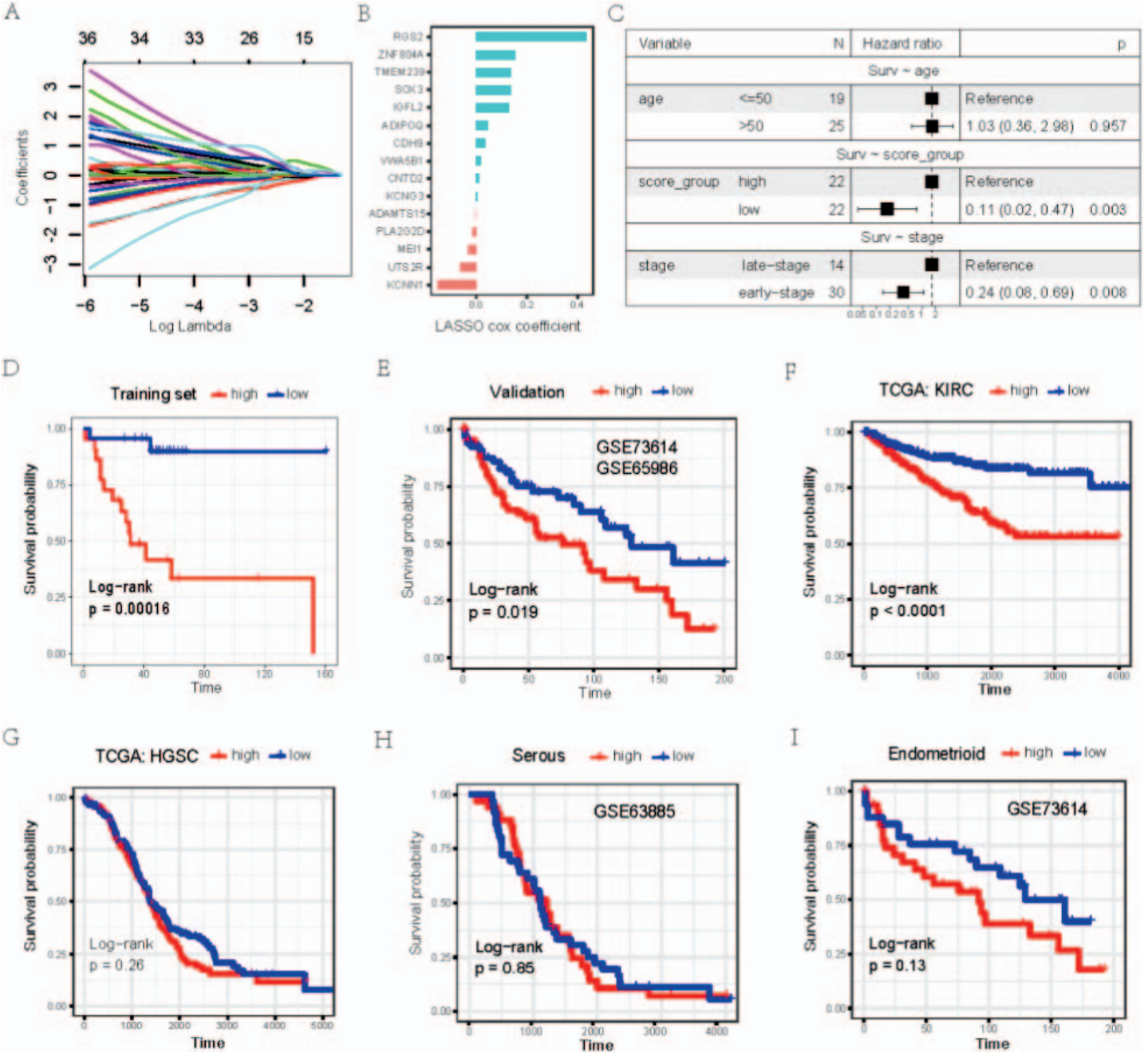

Abstract 26, Figure 4. Establishment and validation of a prognostic immune signature for patients with ovarian clear cell carcinoma (OCCC).

Abstract No: 27

Gender biased clinical and molecular heterogeneity of colorectal cancer liver metastasis: Multi-center propensity analysis of long-term outcomes

Yibin Wu, Lu Wang

Department of Hepatic Surgery, Fudan University Shanghai Cancer Center, Shanghai Medical College, Fudan University, Shanghai, China

Introduction: Cancers of non-reproductive tissue occur in males at a higher frequency and lead to nearly twice the mortality rate compared with these cancers in females. To investigate if male is clinically or genomically distinct from female in colorectal cancer liver metastasis (CLM). **Method:** Retrospectively, 4,912 out of 5,812 patients with CLM were enrolled from 3 participating hospital, and 381 of 1,135 patients were included from a publicly available database, of whom, 3,240 patients underwent curative surgery. All these patients were followed up for over ten years. The

endpoint was overall survival (OS). A 1:1 of propensity score match (PSM) was performed for survival analysis. In addition, 451 human samples (252 male and 199 female) from 3 centers were prospectively analysed by next-generation sequencing (NGS) to describe the gender-biased molecular characteristics of CLM. **Results:** Compared to male, female was more often diagnosed with right colon cancer (29.2% vs 22.6%, P< 0.0001), later stage presented by tumor (T4, 55.2% vs 46.1%, P< 0.0001), node (N1, 34.7% vs 31.8%, P< 0.0001; N2, 30.7% vs 21.7%, P< 0.0001), metastasis staging (M1b/c, 18.4% vs 15.0%, P< 0.0001), and poorer differentiation (29.6% vs 24.6%, P< 0.0001), and more frequent to develop large size of liver metastases (LMs) (20.3% vs 17.3%, P< 0.0001). The survival differences in favor of male were observed in the internal and external validation cohorts regardless of PSM, whose results could be recommended in independent individuals with left (P< 0.0001) or right colon cancer (P < 0.0001), KRAS wild type (P=0.0214) or mutation (P=0.0134), synchronous (P< 0.0001) or metachronous liver metastasis (P < 0.0001), and late-onset disease (P< 0.0001), but not with early-onset disease (P=0.1141). Genetic analysis showed that female patients were more likely to harbor KRAS mutation than male patients. Pathogenic germline variants were identified in 28.2% of male versus 20.5% of female patients. **Conclusion:** There exists gender heterogeneity in CRCLM that determines patients' responses to treatment, including surgery. Integrated somatic and germline mutations help to reveal the gender biased molecular profiles, which lays fundamental evidence for gender-specific cancer prevention and therapeutic strategies

Abstract No: 28

Long noncoding RNA SNHG12 promotes gastric cancer proliferation by binding to HuR and stabilizing YWHAZ expression through the AKT/GSK-3b pathway

Tianqi Zhang

Fudan University Shanghai Cancer Center, Shanghai, China

Introduction: Gastric cancer (GC) is a malignancy with high morbidity and mortality rates worldwide. SNHG12 is a long noncoding RNA (lncRNA) commonly involved many types of cancers in the contexts of tumorigenesis, migration and drug resistance. Nevertheless, its role in GC proliferation is poorly understood. **Method:** Bioinformatics and qRT-PCR assays were used to analyze the expression of SNHG12 in GC tissues and cells. In vitro and in vivo experiments were conducted to detect the role of SNHG12 in GC development. qRT-PCR, PCR, western blotting (WB), RNA binding protein immunoprecipitation (RIP), immunoprecipitation (IP), immunohistochemistry (IHC), fluorescence in situ hybridization (FISH) and in situ hybridization (ISH) were performed to investigate the underlying mechanisms by which SNHG12 promotes GC proliferation**. Results:** SNHG12 was highly expressed in GC cells and tissues, and predicted poor survival. In vitro and in vivo assays showed that SNHG12 knockdown inhibited GC proliferation, while SNHG12 overexpression promoted GC proliferation. Further experiments confirmed that SNHG12 was mainly located in the cytoplasm and bound to HuR. Bioinformatics analysis predicted that YWHAZ was the common target of SNHG12 and HuR, and that the "SNHG12-HuR" complex enhanced the stability of YWHAZ mRNA. Rescue assays verified that SNHG12 promoted GC proliferation by activating the AKT/GSK-3β pathway. **Conclusion:** SNHG12 binds to HuR and stabilizes YWHAZ. SNHG12 promotes GC proliferation via modulation of the YWHAZ/AKT/GSK-3β axis in vitro and in vivo. Thus, SNHG12 could become a novel therapeutic target for anti-tumor therapy.

Abstract No: 29

YY1-modulated long non-coding RNA SNHG12 promotes gastric cancer metastasis by activating the miR-218-5p/YWHAZ axis

Tianqi Zhang

Fudan University Shanghai Cancer Center, Shanghai, China

Introduction: Long non-coding RNA (lncRNA) small nucleolar RNA host gene 12 (SNHG12) plays important roles in the pathogenesis and progression of cancers. However, the role of SNHG12 in the metastasis of gastric cancer (GC) has not yet been thoroughly investigated. **Method**: The SNHG12 expression pattern was detected in GC cell lines, tumor samples from patients with GC using qRT-PCR. In vivo and in vitro assays were conducted to observe the influence of SNHG12 regulation on GC EMT and metastatic potential. The underlying mechanisms were further determined by qRT-PCR, western blotting, dual luciferase reporter assays, immunohistochemistry assays, immunoprecipitation, RIP assays, RNA stability assays, TOPFlash/FOPFlash reporter assays and Ch-IP assays. **Results:** SNHG12 was upregulated in GC tissues and cell lines. In addition, the expression level of SNHG12 in GC samples was significantly related to tumor invasion depth, TNM stage and lymph node metastasis and was associated with disease-free survival (DFS) and overall survival (OS) in patients with GC. In vivo and in vitro assays indicated that SNHG12 promotes GC metastasis and epithelial-mesenchymal transition (EMT). Bioinformatics and mechanistic analyses revealed that SNHG12 can directly target miR-218-5p to regulate YWHAZ mRNA, forming an SNHG12/miR-218- 5p/YWHAZ axis and decreasing the ubiquitination of β-catenin to promote GC metastasis. In addition, SNHG12 stabilizes CTNNB1 mRNA by binding with HuR, thus activating the β-catenin signaling pathway. Further analysis also revealed that the transcription factor YY1 negatively modulates SNHG12

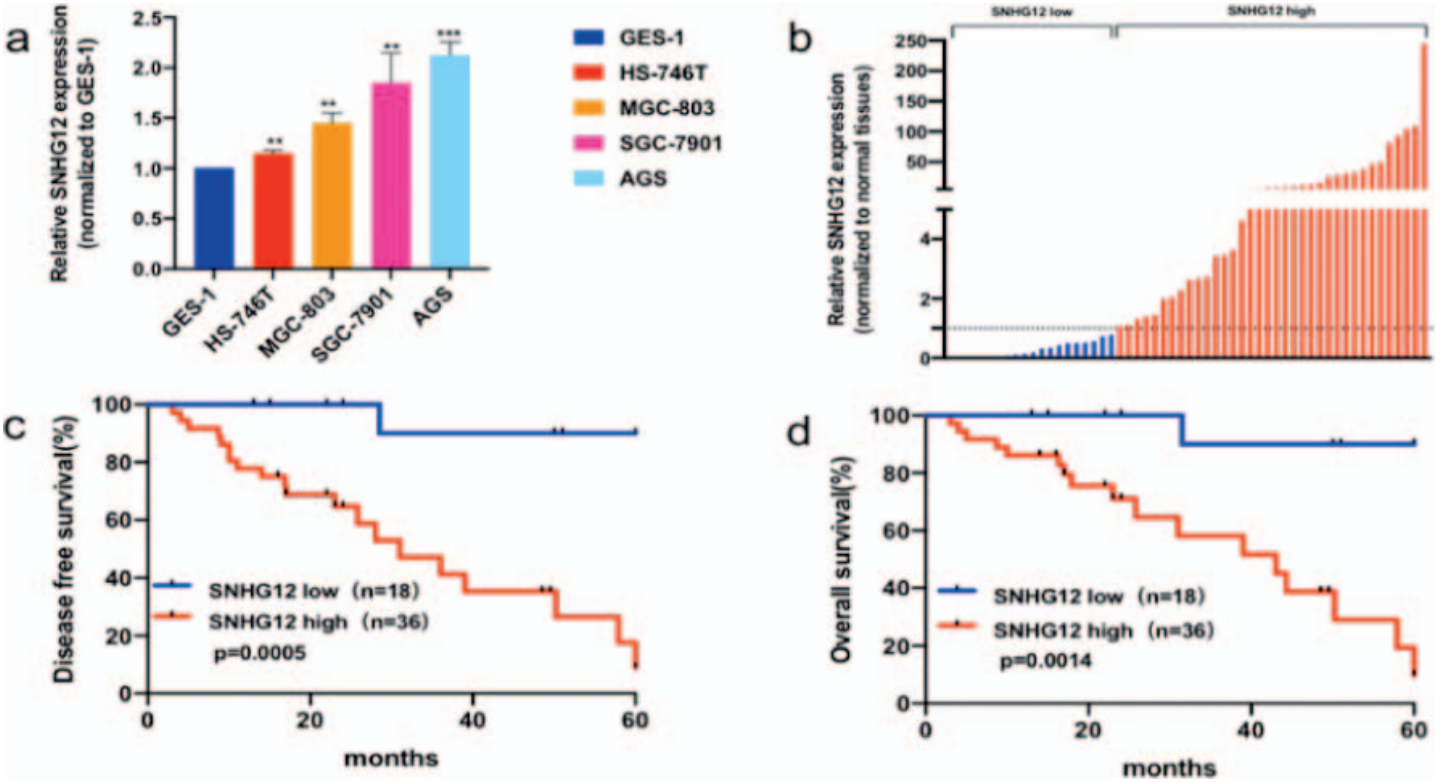

Abstract 29, Figure 1.

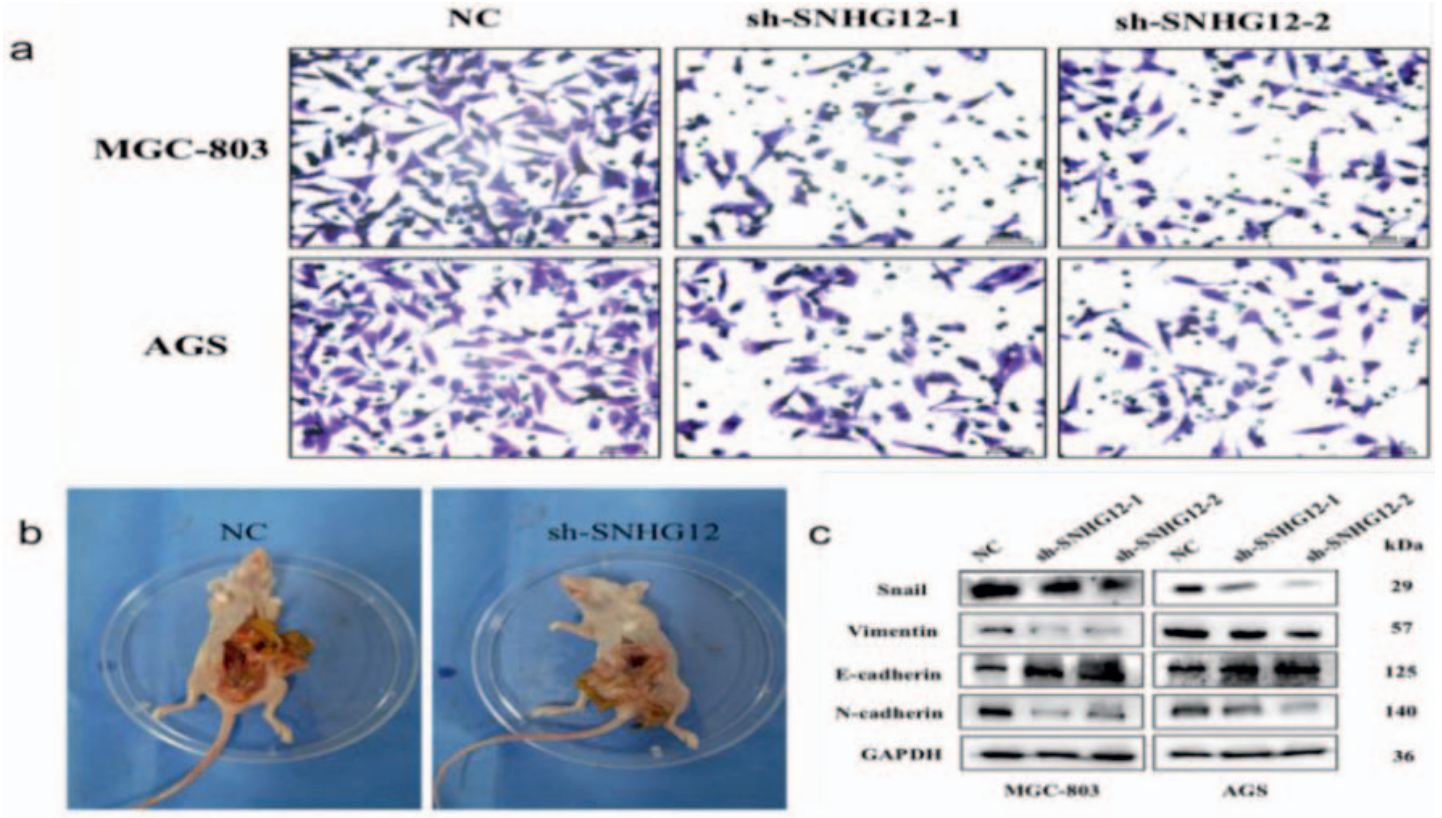

Abstract 29, Figure 2.

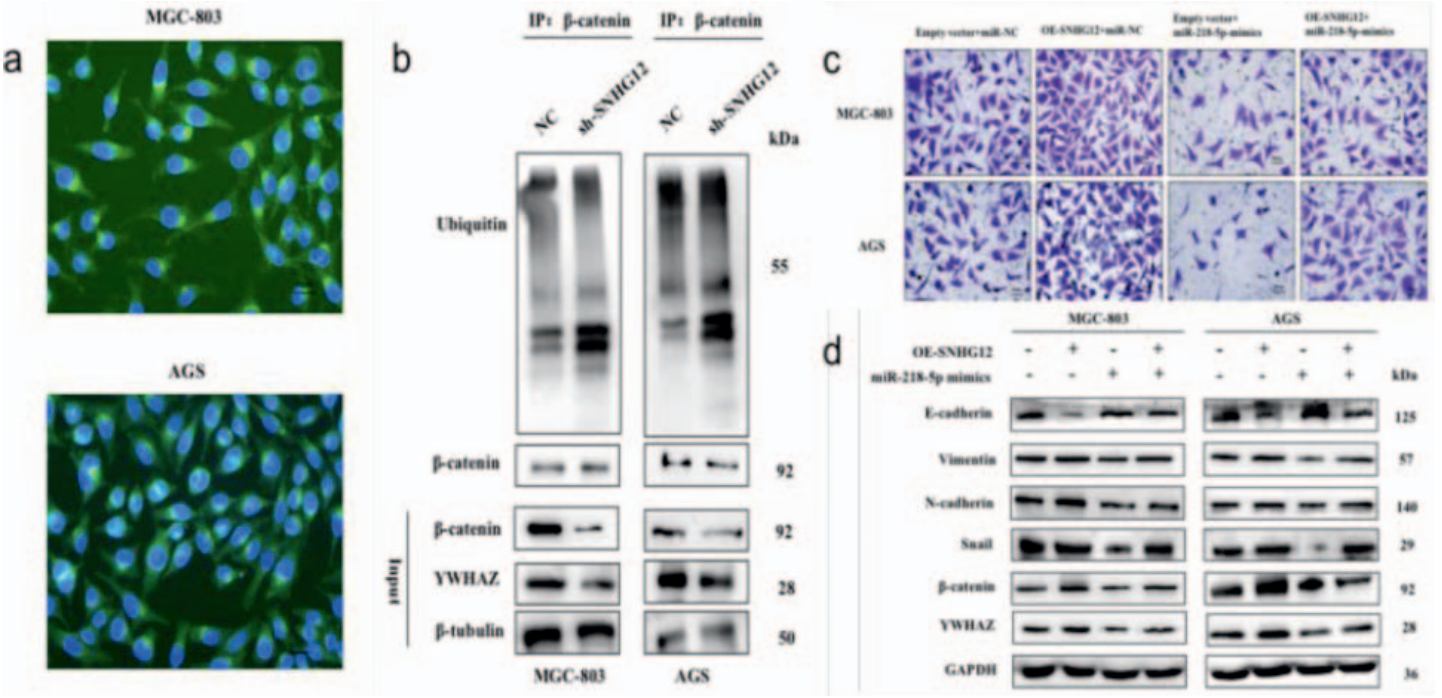

Abstract 29, Figure 3.

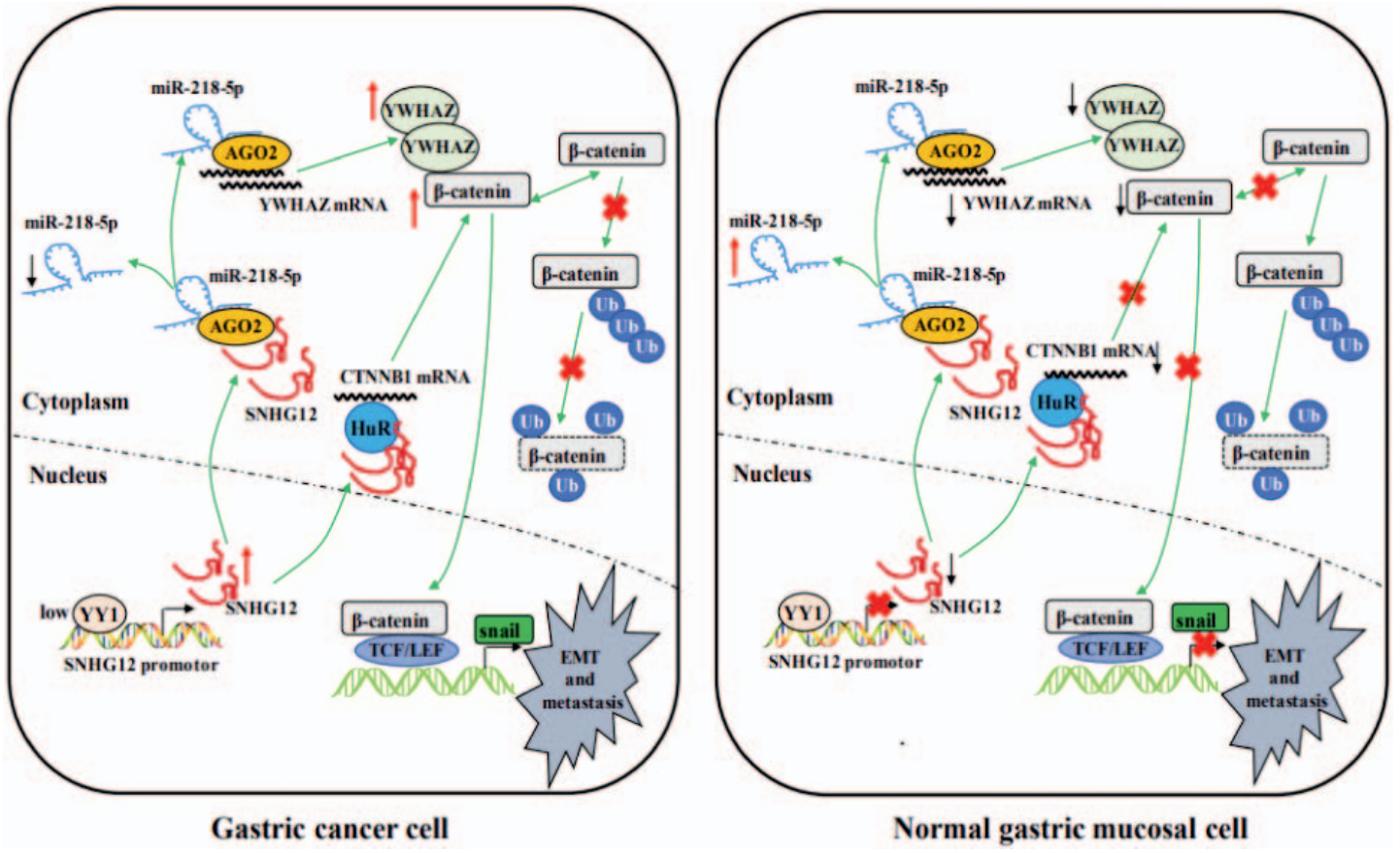

Abstract 29, Figure 4.

transcription. **Conclusion:** SNHG12 is a potential prognostic marker and therapeutic target for GC. Negatively modulated by YY1, SNHG12 promotes GC metastasis and EMT by regulating the miR-218-5p/YWHAZ axis and stabilizing CTNNB1 via activation of the β-catenin signaling pathway.

Abstract No: 30

Circulating tumor DNA in decision-making of patients with metastatic colorectal cancer after failure of first-line treatment containing cetuximab - a single-center, phase II trial

Jianling Zou[1], Wentao Yan[1], Wenhua L[1], Chenchen Wang[1], Xin Hu[2], Zhiyu Chen[1]

[1]Department of Medical Oncology, Fudan University Shanghai Cancer Center, Shanghai, China
[2]Precision Cancer Medicine Center, Department of Breast Surgery, Key Laboratory of Breast Cancer in Shanghai, Fudan University Shanghai Cancer Center, Shanghai, China

Introduction: Cetuximab is a commonly used targeted drug in KRAS, NRAS and BRAF wild type metastatic colorectal cancer (mCRC) and can significantly prolong survival. While the patients' genetic status is constantly changing, so it is important to dynamically monitor patients' genetic status and adjust treatment. We undertook this study to analyze the molecular characteristics of circulating tumor (ctDNA) in patients of RAS and BRAF wild-type mCRC at baseline, who failed after first line treatment containing cetuximab, and to explore the significance of ctDNA-guided individualized second-line targeted therapy strategies. **Method:** Patients with advanced and measurable (RECIST 1.1) mCRC who had RAS and BRAF wild-type genetic status at baseline, and had previously been treated with therapeutic regimen including cetuximab, and recently showed progression on CT/MRI scan were recruited. The patients received ctDNA testing, and different targeted therapy strategies were applied according to gene states of ctDNA as follows: arm A, if there was RAS secondary mutation, the combination of bevacizumab and second-line chemotherapy (such as FOLFOX/XELOX/FOLFIRI/XEIRI/

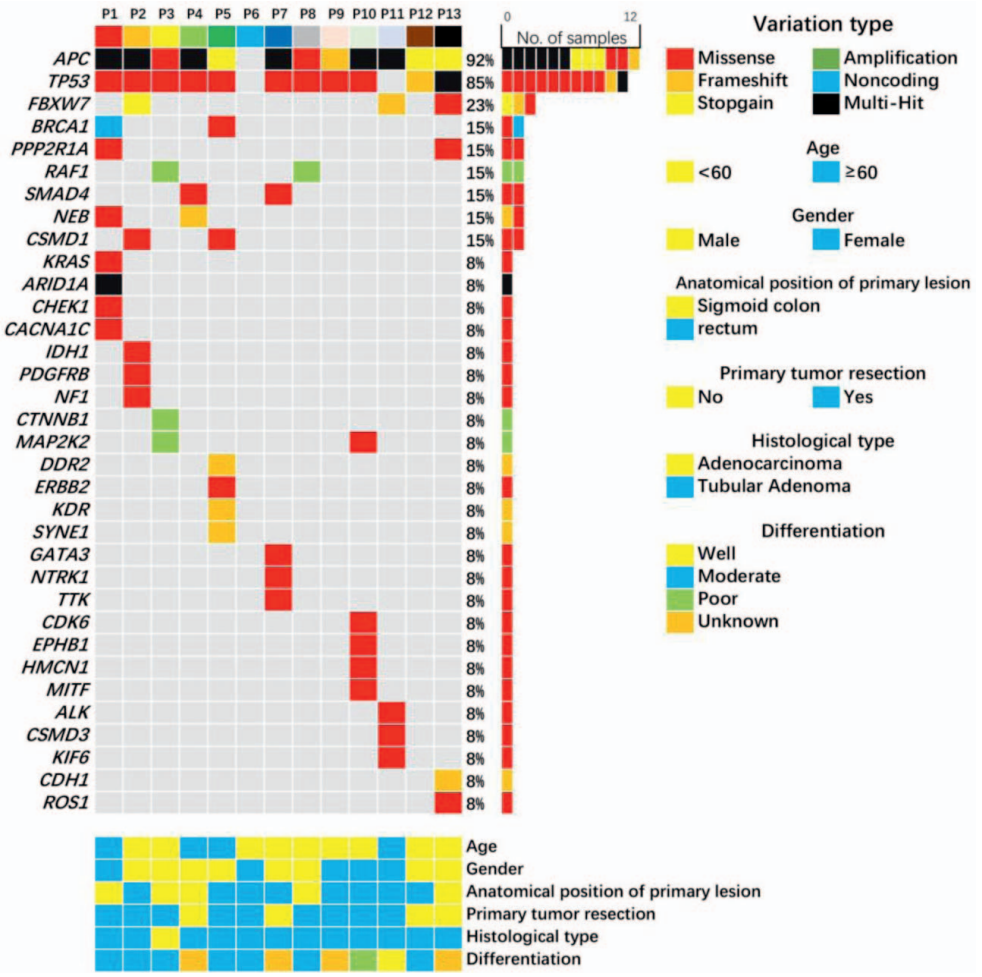

Abstract 30, Figure 1. Genomic profiles before second-line treatment.

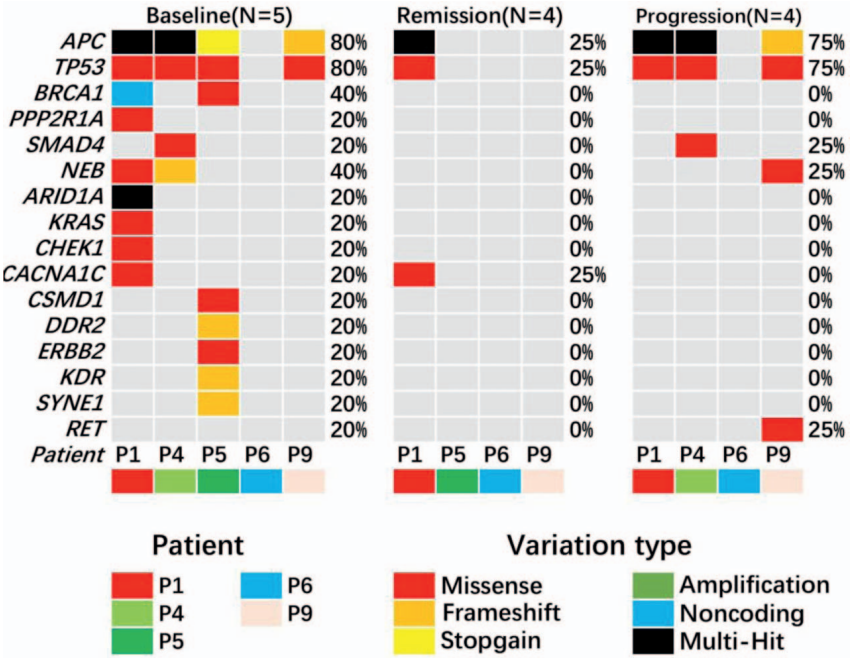

Abstract 30, Figure 2. Dynamic changes in genomic profiles during treatment.

irinotecan, etc.) would be applied ; arm B, if there was BRAF secondary mutation, the combination of vemurafenib, cetuximab and irinotecan would be used; arm C, if HER2 amplification was detected, the combination of trastuzumab and lapatinib/pyrotinib or the combination of trastuzumab and pertuzumab would be used; arm D, if no drug-resistance related secondary variation was found, cetuximab would be applied continuously in combination with second-line chemotherapy (such as FOLFOX/FOLFIRI/ irinotecan monotherapy, etc.). Patients eligible received corresponding therapy regimens and underwent imaging examination and tumor marker detection every 6-8 weeks for efficacy evaluation.

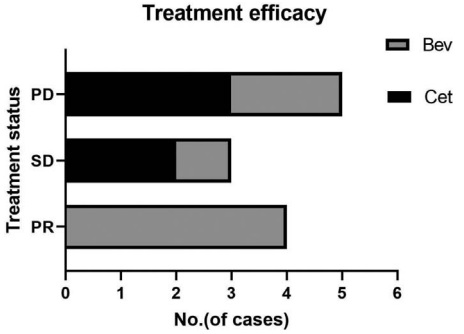

Abstract 30, Figure 3. Treatment efficiency of patients in arm A (bevacizumab-based treatment) and arm D (cetuximab-based treatment).

Primary endpoint was ORR, secondary endpoints were DCR, PFS, OS, quality of life (QLQ-C30), safety and tolerance. **Results:** A total of 13 patients were enrolled (7 in arm A, 0 in arm B, 1 in arm C and 5 in arm D) from April 8, 2021 to Dec 31, 2021. 61.5% (8/13) were males and median age was 51 years. In total, 34 variations were detected in 13 patients before second-line therapy, with a positive rate of 92.3% (12/13). Adenomatous polyposis coli (APC) (92.3%, 12/13) was the most mutated gene, followed by tumor protein 53 (TP53, 84.6%, 11/13) and Fbox/WD repeat-containing protein 7(FBXW7, 23.1%, 3/13). For 4 patients with serial ctDNA detection, the number of gene variation was decreased during disease remission and increased again during progression. For evaluable 11 cases, ORR was 66.7% (4/6) in arm A and 0% (0/5) in arm D (p=n.s.). DCR was 66.7% (4/6) in arm A and 40% (2/5) in arm D (p=n.s.). PFS was unreached in arm A and 4.65 months in arm D (p=n.s.). The OS was unreached in all arms. In addition, no difference in quality of life and treatment related serious adverse advents grade 3-5 was observed. **Conclusion:** Circulating Tumor DNA is a promising biomarker for guiding second-line treatment decisions of patients with mCRC. Though no statistics significance was reached for limited number of cases and follow-up time, the combination of bevacizumab and chemotherapy had the tendency of increased ORR, DCR and PFS than continuously cetuximab based treatment. Further studies are needed to define how to better use ctDNA analysis to guide personalized and risk adjusted therapy strategies in mCRC. Clinical trial information: NCT04831528.

Abstract 30, Table 1.

Characteristics	N (%)
Age (mean and range)	51 (37-63)
⩽60	9 (69.2)
>60	4 (30.8)
Gerder	
Male	8 (61.5)
Female	5 (38.5)
Primary tumor resection	
Yes	9 (69.2)
No	4 (30.8)
Differentiation	
Well	1 (7.7)
Moderate	7(53.8)
Poor	1 (7.7)
Unknown	4 (30.8)
Histological type	
Adenocarcinoma	12 (92.3)
Tubular Adenoma	1 (7.7)
Serum LDH level (U/L, median and range)	308.0 (157.0-1134.0)
<308	6 (46.2)
⩾308	7 (53.8)
Serum CEA level (ng/ml, median and range)	45.9 (2.86-200.0)
<5.4	2 (15.4)
⩾5.4	11 (84.6)
Metastatic sites involved	
⩽1	7 (53.8)
>1	6 (46.2)
Metastatic site	
Liver	11 (84.6)
Lung	6 (46.2)
Bone	2 (15.4)
Others	1 (7.7)
Targeted agent	
Bevacizumab	7 (53.8)
Cetuximab	5 (38.5)
Trastuzumab	1 (7.7)
Combined chemotherapy	
FOLFIRI	9 (69.2)
FOLFOX	2 (15.4)
Irinotecan	1 (7.7))
Pyrotinib Maleate	1 (7.7)

[a]Overall 13 patients were screened for the study.

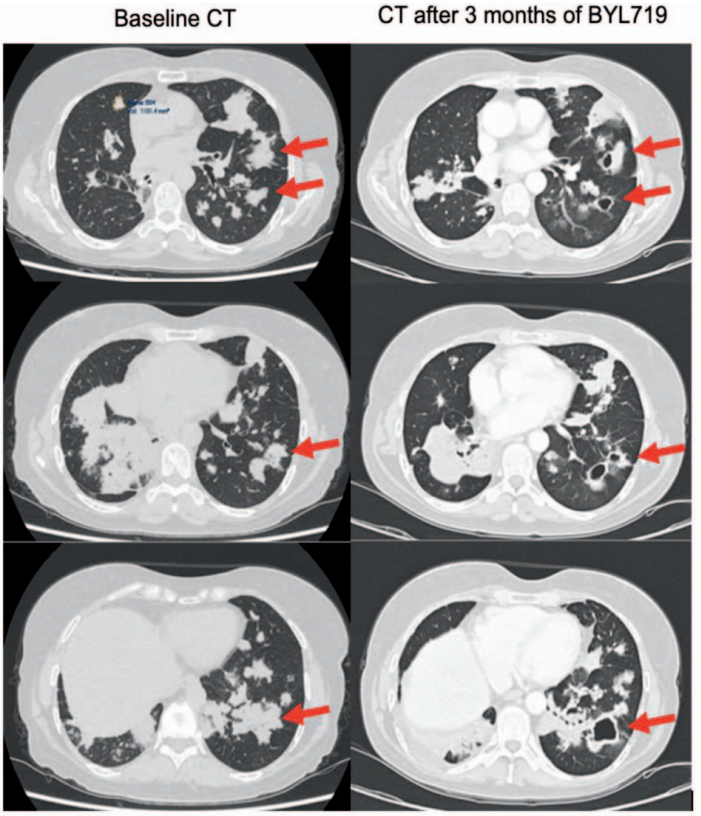

Abstract 31, Figure 1.

Abstract No: 31

Driver mutation characteristics of Phosphatidylinositol-4,5-bisphosphate 3-kinase catalytic subunit alpha (*PIK3CA*) in advanced non-small cell lung cancer

Sameh Daher[1], Rinat Yacobi[2], Roi Tsharnihovsky[3], Iris Barshack[2], Shani Tsabari[4], Yakir Rotenberg[4], Aviad Zick[4], Teodor Gottfried[1], Anastasiya Lobachov[1], Damien Urban[1], Akram Saad[1], Hadas Gantz-Sorotsky[1], Amir Onn[1], Alona Zer[3], Jair Bar[1, 5]

[1]*Thoracic Cancer Unit, Cancer Center, Sheba medical center, Tel HaShomer, Ramat Gan, Israel*
[2]*Institute of pathology, Sheba medical center, Tel HaShomer, Ramat Gan, Israel*
[3]*Davidoff Cancer Center, Rabin Medical Center, Beilinson Campus, Petah Tikva, Israel*
[4]*Sharett Oncology Institute, Hadassah Medical Center, Jerusalem, Israel*
[5]*Tel Aviv University School of Medicine, Tel Aviv, Israel*

Introduction: *PIK3CA* mutations may be driver mutations in non-small cell lung cancer (NSCLC), or simply random co-mutations. We investigated whether patients with NSCLC with *PIK3CA* mutations have driver mutation characteristics. **Methods:** Chart review was performed of patients with advanced NSCLC. Patients with *PIK3CA* mutations were analyzed as two groups: Group A: without any non-PIK3CA established driver mutation; Group B: with coexisting driver mutation. Group A was compared to a cohort of non-*PIK3CA* patients (group C), using t-test and chi-square. To evaluate the impact of *PIK3CA* mutation on outcome, we compared Group A survival to age/sex/histology matched cohort of non-*PIK3CA* mutated patients (group D) by Kaplan-Meier method. A case study of alpelisib-treated solitary *PIK3CA* mutation is reported. **Results:** The total cohort was of 1377 patients, 57 *PIK3CA* mutated (4%). Group A: n-22, group B: n-35. Group A median age was 76 years, 16 (72.7%) men, 10 (45.5%) squamous, 4 (18.2%) never smokers. Two never-smoker females with adenocarcinoma had solitary *PIK3CA* mutation. One of them was treated with a PI3Ka-isoform selective inhibitor BYL719 (Alpelisib), with rapid clinical and partial radiological improvement. Group B, compared with Group A, included younger patients (p=0.03), more females (p=0.03) and more adenocarcinoma cases (p<0.001). Group A patients were older (p=0.03) and had more squamous histology (p=0.01) than group C. Group A showed a trend of longer survival than group D (12 vs. 7 months, p=0.85). **Conclusion**: In most patients with NSCLC with *PIK3CA* mutation there are no characteristics of a driver mutation. *PIK3CA* mutation may be a driver when present as a solitary mutation.

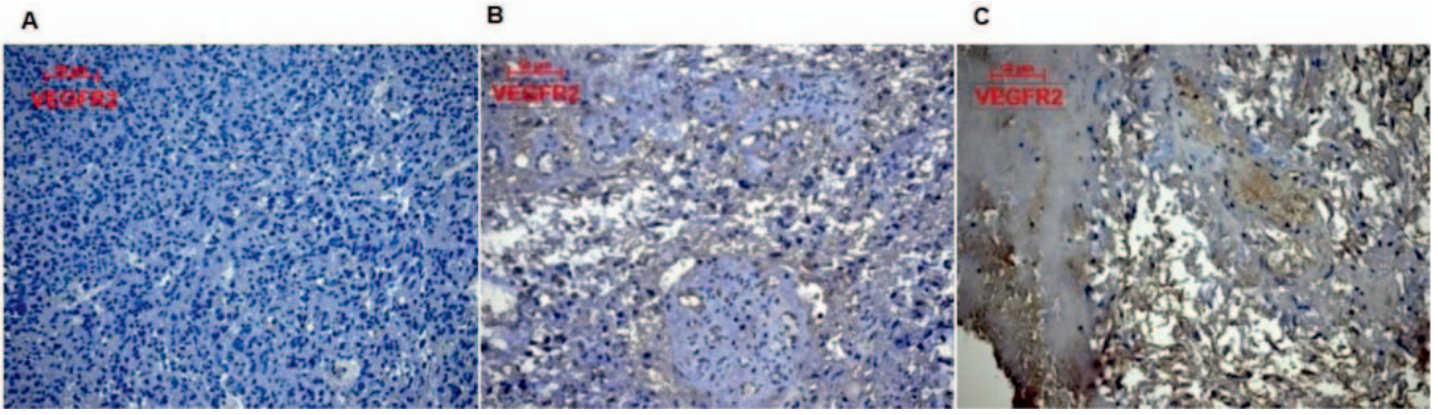

Abstract 32, Figure 1. VEGFR expression in glioblastoma tissues. No VEGFR staining (1A): Moderate VEGFR (1B); Intense VEGFR staining (1C).

Abstract No: 32

VEGFR as a predictive biomarker to anti-angiogenic therapy in glioblastoma

Alexandru Oprita, Ani Simona Sevastre, Daniela Elise Tache, Stefan Alexandru Artene, Oana Alexandru, Ligia Gabriela Tataranu, Anica Dricu

University of Medicine and Pharmacy of Craiova, Craiova, Romania

Introduction: Due to their clinical relevance, cancer biomarkers are therapeutic targets for glioblastoma (GB), the most lethal malignant tumor of the central nervous system, with a median survival less than 15 months. Pathological angiogenesis plays a key role in the development, growth and progression of GB and is supported by a number of growth factor receptors, including vascular endothelial growth factor receptor (VEGFR). In this study, surgically excised GB tissues were examined for the expression of VEGFR. The next goal of our study was to analyze how VEGFR inhibition influences GB cells viability *in vitro*. Using sorafenib (SRFN) and axitinib (AXT), two VEGFR inhibitors approved by Food and Drug Administration (FDA), we also analyzed the effect of receptor inactivation on GB cells viability. **Methods:** GB tumor specimens were obtained from 37 patients operated at Bagdasar Arseny Emergency Hospital in Bucharest, in the department of neurosurgery, between 2008 and 2012 (ethical approval was obtained for this study). Of all GB cases, about 76% were newly diagnosed and 24% were recurrent. GB tumor tissues have been routinely formalin fixed for 72 h and then paraffin embedded. VEGFR expression in the resected GB tissues was evaluated by immunohistochemistry (IHC). The GB1B cell line used in this study was established in our laboratory, from brain tumor fresh samples, collected from patients with brain tumors operated at the "Bagdasar-Arseni" Emergency Hospital, Bucharest, Romania. The cells were grown in standard DMEM enriched with 10% FBS, 2 mM glutamine and a

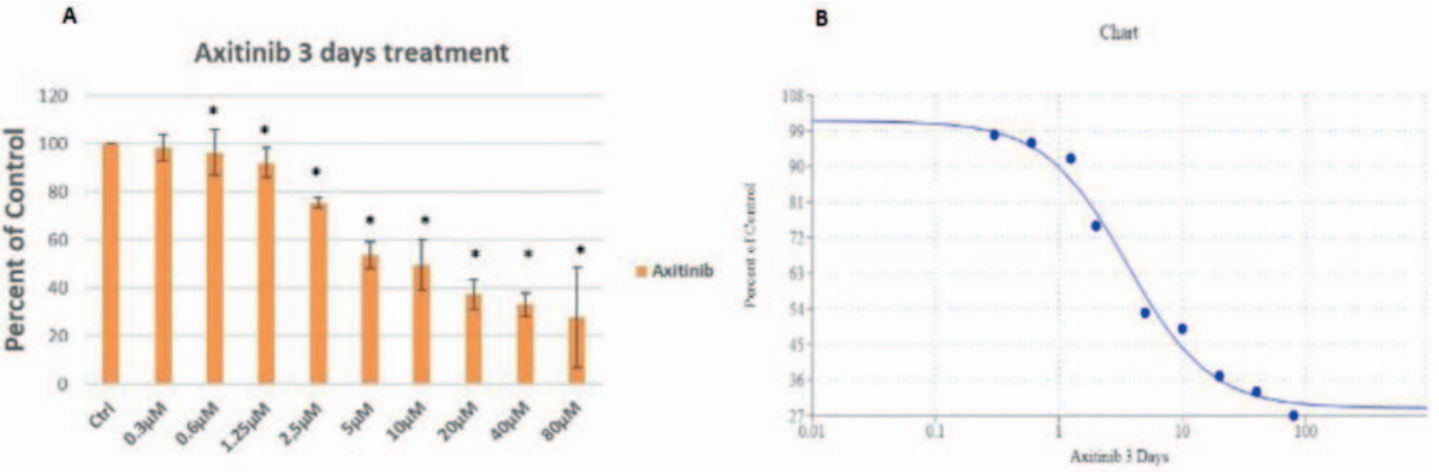

Abstract 32, Figure 2. The effect of Axitinib on GB1B proliferation (A) and the calibration curves for $IC^{50(B)}$ at 3 days of treatment. Results are expressed as percentage of control. Data represents the mean and standard error of 3 separate experiments. Error bars are the mean ± SD for each drug concentration, representing the linear model fit to the data.

*Represents significant difference from control ($p<0.05$).

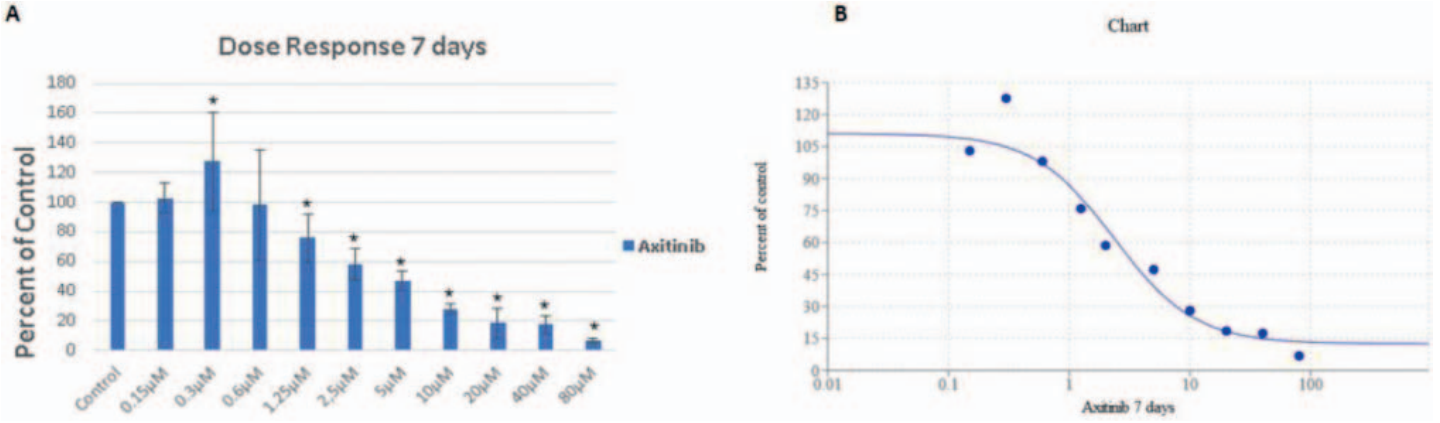

Abstract 32, Figure 3. The effect of Axitinib on GB1B proliferation (A) and the calibration curves for $IC^{50(B)}$ at 7 days of treatment. Results are expressed as percentage of control. Data represents the mean and standard error of 3 separate experiments. Error bars are the mean ± SD for each drug concentration, representing the linear model fit to the data.

*Represents significant difference from control ($p<0.05$).

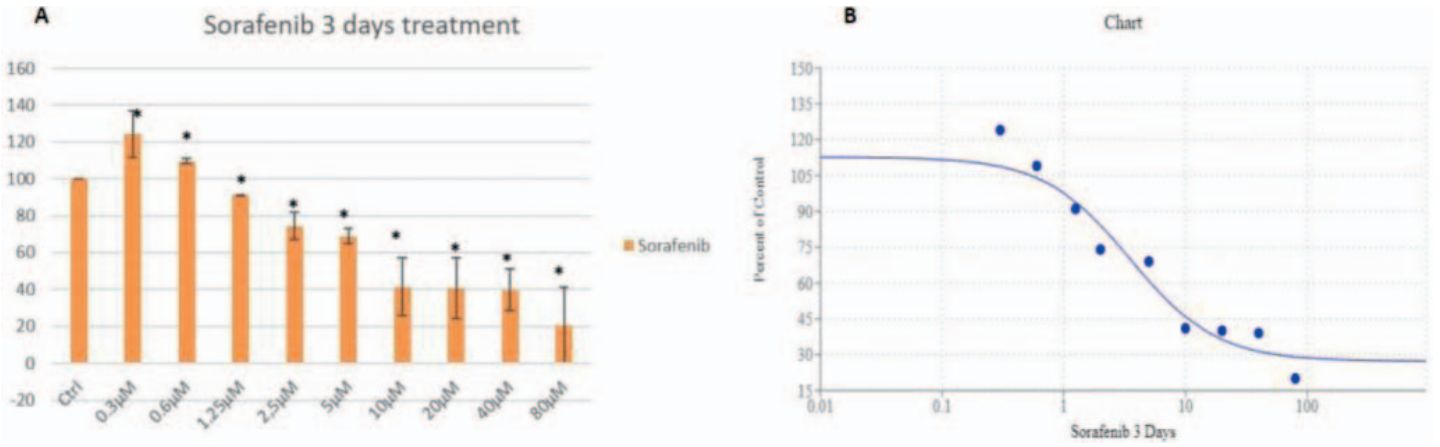

Abstract 32, Figure 4. The effect of Sorafenib on GB1B proliferation (A) and the calibration curves for IC^{50} (B) at 3 days of treatment. Results are expressed as percentage of control. Data represents the mean and standard error of 3 separate experiments. Error bars are the mean ± SD for each drug concentration, representing the linear model fit to the data.

*Represents significant difference from control ($p<0.05$).

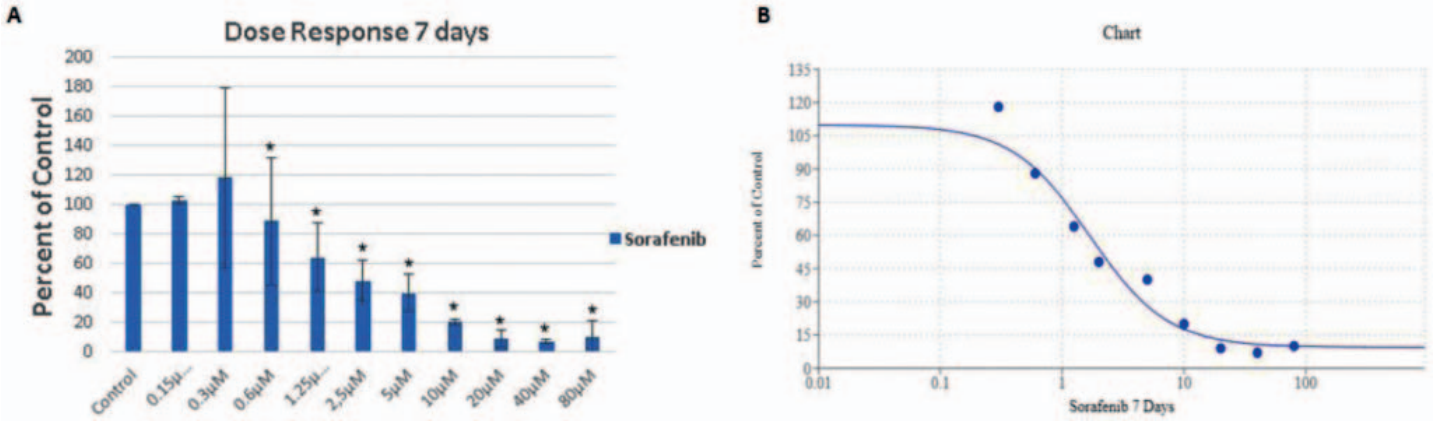

Abstract 32, Figure 5. The effect of Sorafenib on GB1B proliferation (A) and the calibration curves for IC^{50} (B) at 7 days of treatment. Results are expressed as percentage of control. Data represents the mean and standard error of 3 separate experiments. Error bars are the mean ± SD for each drug concentration, representing the linear model fit to the data.

*Represents significant difference from control ($p<0.05$).

combination of two antibiotics (100 IU/mL penicillin and 100 IU/mL streptomycin). For the experiments, cells were seeded in 96-well plates (1-3×10^3 cells/well) and treated with SRFN and AXT, at concentrations varying from 0,3 μM to 80 μM. Every two days, the drugs were refreshed in the culture medium. The effect of VEGFR inactivation on HGG cell lines was evaluated by MTT assay**.** Control groups treated with solvents only were included. For each data point, the experiments were conducted in triplicate or quadruplicate. The formula to estimate the inhibitory concentration that leads to death of 50% of cells (IC_{50}) was calculated with the free online Quest Graph™ IC_{50} Calculator, provided by www.aatbio.com**. Results:** Our results showed that 89% of all GB tumors were positive for VEGFR2**.** The percent of recurrent GB tumors that expressed VEGFR2 was also 89%. IHC analysis revealed no significant differences in receptor expression between newly diagnosed and recurrent GB tumors. An example of VEGFR staining is shown in Fig 1. As shown in Fig 2, both AXT and SRFN reduced GB1B cell growth in a dose- and time-dependent manner, as compared with untreated control groups. After 3 days, in the GB1B cell line, exposure to progressive AXT concentration produced the following significant results: 1.25μM decreased cell viability by 8%, 2.5μM decreased cell viability by 25%, 5μM decreased cell viability by 47%, 10μM decreased cell viability by 51%, 20μM decreased cell viability by 63%, 40μM decreased cell viability by 66% and 80μM reduced cell proliferation by 73%. (Figure 2A). Prolonged exposure of GB1B cells to 7 days treatment with progressive AXT concentration resulted in higher cytotoxicity: 1.25μM decreased cell viability by 25%, 2.5μM decreased cell viability by 42%, 5μM decreased cell viability by 53%, 10μM decreased cell viability by 72%, 20μM decreased cell, viability by 92%, 40μM decreased cell viability by 93% and 80μM reduced cell proliferation by 97% (Figure 3A). The IC_{50}value for AXT was 3.6μM at 3 days of treatment (Figure 2B) and 2.2μM at 7 days of treatment (Figure 3B). The decrease in percentage of viable cells after 3 days treatment with SRFN was: 9% at the drug concentration 1.25μM, 25% when *cells* were treated with 2.5μM, 41%, when *cells* were treated with 5μM, 59%, when *cells* were treated with 10μM, 60%, when *cells* were treated with 20μM, 61% when cells were treated with 40μM and 80%, when cells were treated with 80μM (Figure 4A). The viability of the cells decreased further after 7 days of treatment with SRFN, causing 46% cell death after treatment with1.25μM, 52% cell death after treatment with 2.5μM, 60% cell death after treatment with 5μM, 80% cell death after treatment with 10μM, 91% cell death after treatment with 20μM, 93% cell death after treatment with 40μM and 90% cell death after treatment with 80μM (Figure 5A). The IC_{50}value for SRFN was 3.5μM at 3 days of treatment (Figure 4B) and 1.7μM at 7 days of treatment (Figure 5B). Collectively, our results indicate that GB express VEGFR and may serve as an important target in GB treatment. **Conclusion:** A profound understanding of molecular basis of glioblastoma can lead to the diagnostic, predictive, prognostic, and therapeutic biomarkers. Identifying biomarkers may increase chance of survival for patients with glioblastoma as they will enable early diagnosis and also guide the choice of a targeted therapy.

Abstract No: 33

New potential therapeutic strategies in lung cancer using obatoclax mesylate

Ancuta Jurj, Cornelia Braicu, Oana Zanoaga, Lajos Raduly, Cristina Ciocan, Ioana Berindan-Neagoe

Research Center for Functional Genomics, Biomedicine and Translational Medicine, Iuliu Haţieganu University of Medicine and Pharmacy, Cluj-Napoca, Romania

Introduction: Lung adenocarcinoma is one of the most frequent malignancies worldwide in both men and women. New therapeutic approaches are needed to improve the treatment of lung adenocarcinoma. Because of this, the aim of the current study was to determine the effects of Obatoclax on lung adenocarcinoma cell lines. **Methods:** The cell lines used in the current study were BEAS-2B (normal lung cell line), and H522, and H1792 (lung adenocarcinoma cell lines). All functional assays and transcriptomic evaluation were performed on using a 0.8μM Obatoclax concentration. **Results:** We first performed MTT assay at 48 hours for both H1792 and H522 cell lines to determine the optimal concentration of Obatoclax which will be used for further experiments. Then, using the previously selected Obatoclax Mesylate dose, we assessed altered cellular processes using fluorescence microscopy. We analyzed the migration rate of the treated cells and observed a reduced migration in the Obatoclax condition compared to the untreated counterparts. To determine if the expression profiles of these cells are affected by Obatoclax, we assessed both protein-coding gene expression and long noncoding RNA expression through microarray. Through this we observed that BEAS-2B cell line had significantly fewer altered genes between the conditions and that there were 6 upregulated and 2 downregulated transcripts that were significantly different in the Obatoclax treated lung adenocarcinoma cell lines compared to their untreated counterparts. **Conclusion:** In the current study we have shown that Obatoclax had a significant effect on lung adenocarcinoma cell lines than on a normal epithelial cell line considering cell proliferation, migration and the expression differences generated by Obatoclax Mesylate.

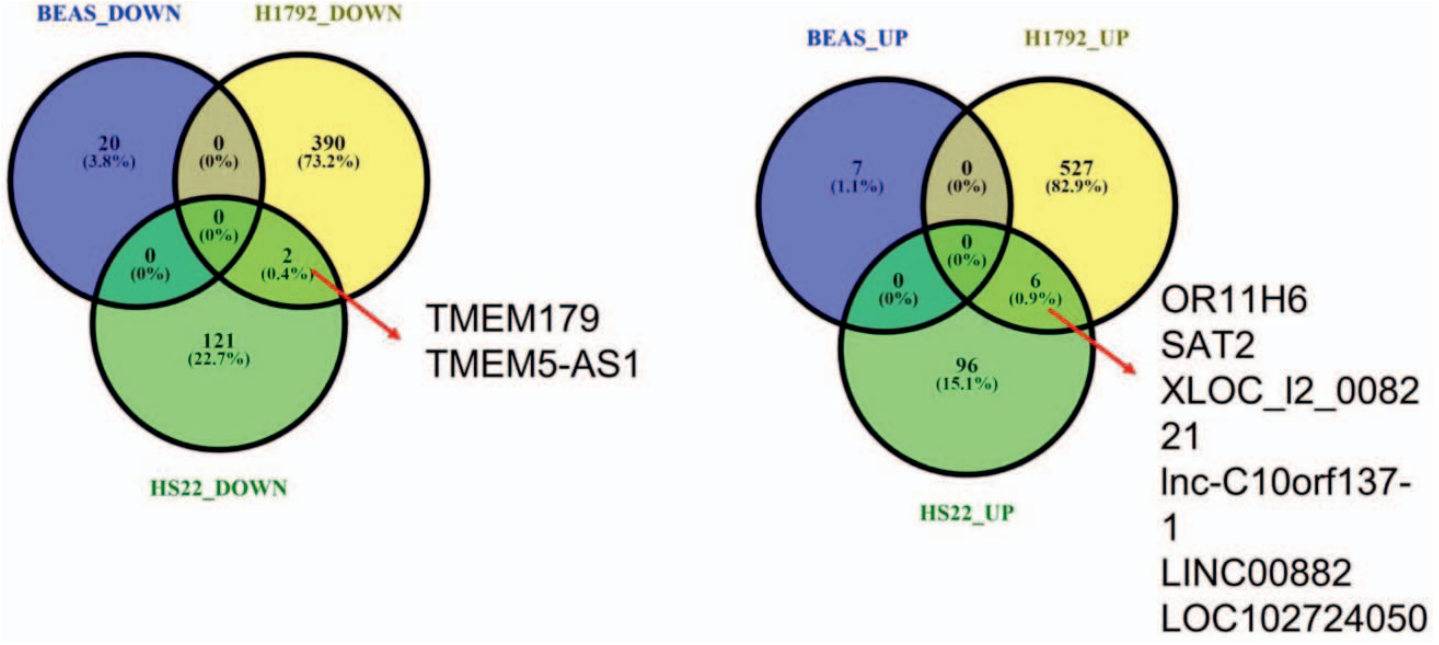

Abstract 33, Figure 1. The common genes and lncRNAs between H522 and H1792, but not altered in BEAS-2B.